

AD-A106 283

AIR FORCE INST OF TECH WRIGHT-PATTERSON AFB OH
A PHOTOLUMINESCENCE STUDY OF DEFECTS IN GAAS CAUSED BY FILM DEP--ETC(U)
1978 J A BOWDEN
AFIT-CI-79-260T

F/O 7/4

UNCLASSIFIED

NL

1 - 1
2 - 2

END
DATE
FILMED
11 81
DTIC

LEVEL II

①

79-667

THESIS

AD A106283

A PHOTOLUMINESCENCE STUDY OF
DEFECTS IN GaAs CAUSED BY
FILM DEPOSITION AND ANNEALING

Submitted by
Joseph A. Bowden
Physics Department

ADTIC
ELEC
S OCT 29 1981

E

DTIC FILE COPY

In partial fulfillment of the requirements
for the Degree of Master of Science
Colorado State University
Fort Collins, Colorado
Fall, 1978

UNCLASS

SECURITY CLASSIFICATION OF THIS PAGE (When Data Entered)

REPORT DOCUMENTATION PAGE		READ INSTRUCTIONS BEFORE COMPLETING FORM
1. REPORT NUMBER 79-260T	2. GOVT ACCESSION NO. AD-A106	3. RECIPIENT'S CATALOG NUMBER 283
4. TITLE (and Subtitle) A Photoluminescence Study of Defects in GaAs Caused by Film Deposition and Annealing		5. TYPE OF REPORT & PERIOD COVERED THESIS/D19999747104
7. AUTHOR(s) Joseph A. Bowden		6. PERFORMING ORG. REPORT NUMBER
9. PERFORMING ORGANIZATION NAME AND ADDRESS AFIT STUDENT AT: Colorado State University		8. CONTRACT OR GRANT NUMBER(s) 11 711
11. CONTROLLING OFFICE NAME AND ADDRESS AFIT/NK WPAFB OH 45433		10. PROGRAM ELEMENT, PROJECT, TASK AREA & WORK UNIT NUMBERS
12. REPORT DATE Fall 1978		13. NUMBER OF PAGES 70
14. MONITORING AGENCY NAME & ADDRESS (if different from Controlling Office)		15. SECURITY CLASS. (of this report) UNCLASS
16. DISTRIBUTION STATEMENT (of this Report) APPROVED FOR PUBLIC RELEASE; DISTRIBUTION UNLIMITED		
17. DISTRIBUTION STATEMENT (of the abstract entered in Block 20, if different from Report)		
18. SUPPLEMENTARY NOTES APPROVED FOR PUBLIC RELEASE: IAW AFR 190-17		20 OCT 1981 Fredric C. Lynch FREDRIC C. LYNCH, Major, USAF Director of Public Affairs Air Force Institute of Technology (AFIT) Wright-Patterson AFB, OH 45433
19. KEY WORDS (Continue on reverse side if necessary and identify by block number)		
20. ABSTRACT (Continue on reverse side if necessary and identify by block number) ATTACHED 81 10 26 221		

COLORADO STATE UNIVERSITY

Fall 1978

WE HEREBY RECOMMEND THAT THE THESIS PREPARED UNDER OUR
SUPERVISION BY JOSEPH A. BOWDEN
ENTITLED A PHOTOLUMINESCENCE STUDY OF DEFECTS IN GaAs
CAUSED BY FILM DEPOSITION AND ANNEALING
BE ACCEPTED AS FULFILLING IN PART REQUIREMENTS FOR THE
DEGREE OF MASTER OF SCIENCE

Committee on Graduate Work

H. H. Wieder

H. H. Wieder/IRS

James R. Sites

Adviser

Accession No.	
Project	
Subject	
Author	
J.	
P.	
State	
Address	
City	
Dist.	
Special	
A	

79-2601

ABSTRACT OF THESIS

A PHOTOLUMINESCENCE STUDY OF DEFECTS IN GaAs CAUSED BY FILM DEPOSITION AND ANNEALING

Photoluminescence (PL) is used to investigate changes induced in the surface layer of a Gallium Arsenide (GaAs) substrate by sputter-deposition and subsequent annealing. Since PL is both sensitive and non-destructive, it provides a powerful research tool for investigating optically active defects and impurities at near band gap energies. Emission spectra of GaAs substrates encapsulated with thin films of silicon nitride (Si_3N_4) by the technique of neutralized ion beam sputter-deposition reveal no optically active defects at near band gap energies. Annealing substrates encapsulated with Si_3N_4 adds an emission to the PL spectrum. This emission is attributed to a Gallium vacancy (V_{Ga})-Silicon acceptor complex. This same complex may also be generated during annealing of bare GaAs substrates doped with Silicon (Si). This complex acts to compensate a n-type surface layer of the substrate and, in general, degrades its qualities.

Joseph A. Bowden
Physics Department
Colorado State University
Fort Collins, Colorado 80523
Fall, 1978

TABLE OF CONTENTS

	<u>Page</u>
ABSTRACT	iii
LIST OF FIGURES	v
Chapter 1. INTRODUCTION	1
Chapter 2. PHOTOLUMINESCENCE	4
A. Background and Transitions	4
B. History	9
C. Theory	11
Chapter 3. DATA-TAKING AND SUBSTRATE PREPARATION.	14
A. Apparatus and Data-Taking Pro- cedures	14
B. Sample Preparation and Encap- sulation	22
Chapter 4. DATA ANALYSIS	27
A. Bare Substrate Analysis	27
B. Encapsulation and Annealing	48
C. Observations on Encapsulation and Annealing	56
Chapter 5. CONCLUSIONS	66
BIBLIOGRAPHY	70

LIST OF FIGURES

<u>Figure</u>		<u>Page</u>
2-1	Optical transitions	7
3-1	Janis Cryogenic dewar	15
3-2	Photoluminescence apparatus	18
3-3	Relative spectra response of Si p-i-n diode	21
3-4	Neutralized ion beam sputter-deposition apparatus	24
4-1	Sample J-1	31
4-2	Variation of GaAs band gap energy with temperature	33
4-3	Williams' configuration-coordinate model .	40
4-4	Summary of transitions, Sample J-1	40
4-5	Sample L-2	45
4-6	Sample GaAs: Si	47
4-7	Si ₃ N ₄ deposition techniques	51
4-8	PL spectra at 6°K	52
4-9	Samples J-2, L-7	58
4-10	Sample J-3	61
4-11	Samples L-3, N-3	64

CHAPTER I

Gallium Arsenide (GaAs) is a compound semiconductor that crystallizes in the zincblende lattice structure and has a direct energy gap. Because of its high mobility and direct band gap, GaAs has attracted attention for special applications in microwave devices, light-emitting diodes, and solid state lasers. To be able to fabricate these specialized devices, though, we must understand the behavior of GaAs throughout its entire range of use: from crystal growth to device fabrication to product use. Since it is well known that heat treatment of GaAs introduces lattice damage at temperatures greater than approximately 400°C, we must thoroughly understand the process that causes the damage so that we may accurately control the quality of GaAs semiconductor devices.

This thesis seeks to further the understanding of the damage caused during the encapsulation and annealing of GaAs substrates. Encapsulation is the deposition of a dielectric film for the purpose of suppressing out diffusion of Arsenic (As) during ion implantation annealing in GaAs device technology. Annealing is performed either concurrently with or after ion implantation in order to repair lattice damage from the impact of high energy particles and to assure that implanted atoms are incorporated into electrically active sites. Both encapsulation and annealing can involve

temperatures great enough to cause significant changes to the electrical and optical properties of the substrate.

I intend to use a research technique known as Photoluminescence (PL) to study the optical emission spectra of substrates that have been encapsulated and annealed. These recorded spectra will then be compared to the spectra of untreated substrates for changes induced by silicon nitride (Si_3N_4) film deposition and annealing. It will be important to study the PL spectra of encapsulated, unannealed substrates for damage caused by the deposition process. We must be able to distinguish deposition and annealing effects so that annealing related defect emissions can be identified. Spectral emission lines will be analyzed in terms of known substitutional impurities and defects. Finally, I will attempt to identify the cause of deposition and annealing defects and describe their formation process.

My thesis will be presented in five chapters. This chapter, one, gives a motivation for investigating the behavior of GaAs during heat treatment. Chapter two introduces the PL process: optical transitions, a short history of the PL of GaAs, and a very brief description of the theory of PL. In Chapter three, I describe the PL apparatus and the encapsulation technique. Chapter four presents the recorded emission spectra and their analysis. In Chapter five, I present my conclusions concerning the identity and formation process of deposition and annealing defects in our GaAs samples.

My thesis is intended to give the reader an understanding of the assumed defect formation process in bare and encapsulated substrates that have been annealed. This process must either be controlled or exploited if the semiconductor industry is to provide specialized devices that utilize the unique qualities of GaAs to their fullest potential.

CHAPTER II

Because we are going to use PL to investigate the optically radiative defects caused during encapsulation and annealing, it is necessary to give some background into this research technique. First, I will give a brief overview of PL, its advantages and drawbacks, and the most important energy band transitions that we will observe by this process. Next, I will give a short history of the PL of GaAs. Finally, I will explain a particular theory of radiative emission in GaAs that allows us to understand the probabilities of band transitions in terms of carrier lifetime and concentration. This chapter is meant to furnish the reader with sufficient background to understand the transitions seen in chapter four.

A. Background and Transitions

PL is the optical radiation emitted by a physical system resulting from excitation to a non-equilibrium state by irradiation with light. Three separate steps in the luminescence process can be distinguished: the creation of electron-hole pairs (EHP's) by absorption of the exciting light, radiative recombination of EHP's, and the escape of the recombination radiation from the sample.

Since the exciting light is absorbed in creating EHP's, the greatest excitation of the sample is near the surface; the resulting non-equilibrium carrier distribution is, hence, inhomogeneous in the direction normal to the surface. In attempting to regain homogeneity and equilibrium, the excess carriers diffuse away from the surface while being depleted by both radiative and non-radiative recombination processes. Most of the excitation of the crystal is restricted to a region within a diffusion length of the surface. Therefore, most of the recombination radiation will escape directly through the surface, and thus, most of the PL experiments are arranged to examine light emitted from the irradiated side of the sample.

As with any other method of scientific investigation, PL presents several advantages and disadvantages for its use. There are two primary reasons why PL is being used as a research tool that is comparable in importance to absorption measurements. First, it is a very sensitive technique; impurities and defects in GaAs which are present in concentrations as small as $\sim 10^{15} \text{ cm}^{-3}$ can be detected without destruction of the sample. The second reason is the simplicity of data collection; special sample preparation is not necessary for PL and surface irregularities are generally unimportant. The most significant drawback is the difficulty of interpreting the data. Conclusive results

are often very difficult to obtain. PL combined with electronic measurements, however, presents the researcher with a very powerful tool. It is best used to complement other methods of investigation, but it is still a very successful technique in its own right.

In order to identify defects and impurities in substrates, we must study the optical emissions which the non-equilibrium excitation causes. There are five basic optical transitions which will be seen in our samples: conduction band to valence band (B-B), conduction band to acceptor level (B-A), donor level to valence band (D-B), free exciton recombination, and donor level to acceptor level (D-A) or pair transitions. These are shown in Fig (2-1).

(B-B) recombination occurs when a conduction electron occupies an empty bond in the GaAs lattice and gives up an energy equal to the gap energy (E_g) of the crystal. (B-A) transitions occur when a conduction electron occupies the empty bond provided by a substitutional acceptor; essentially, the acceptor becomes ionized and gives up a photon of energy ($E_g - E_A$) where E_A , the ionization energy of the hole, is measured from the valence band. (D-B) transitions occur when the donor conduction electron occupies an empty bond (a hole) in the GaAs lattice.

A free hole and a free electron as a pair of opposite charges experience a coulomb attraction. Hence, the electron

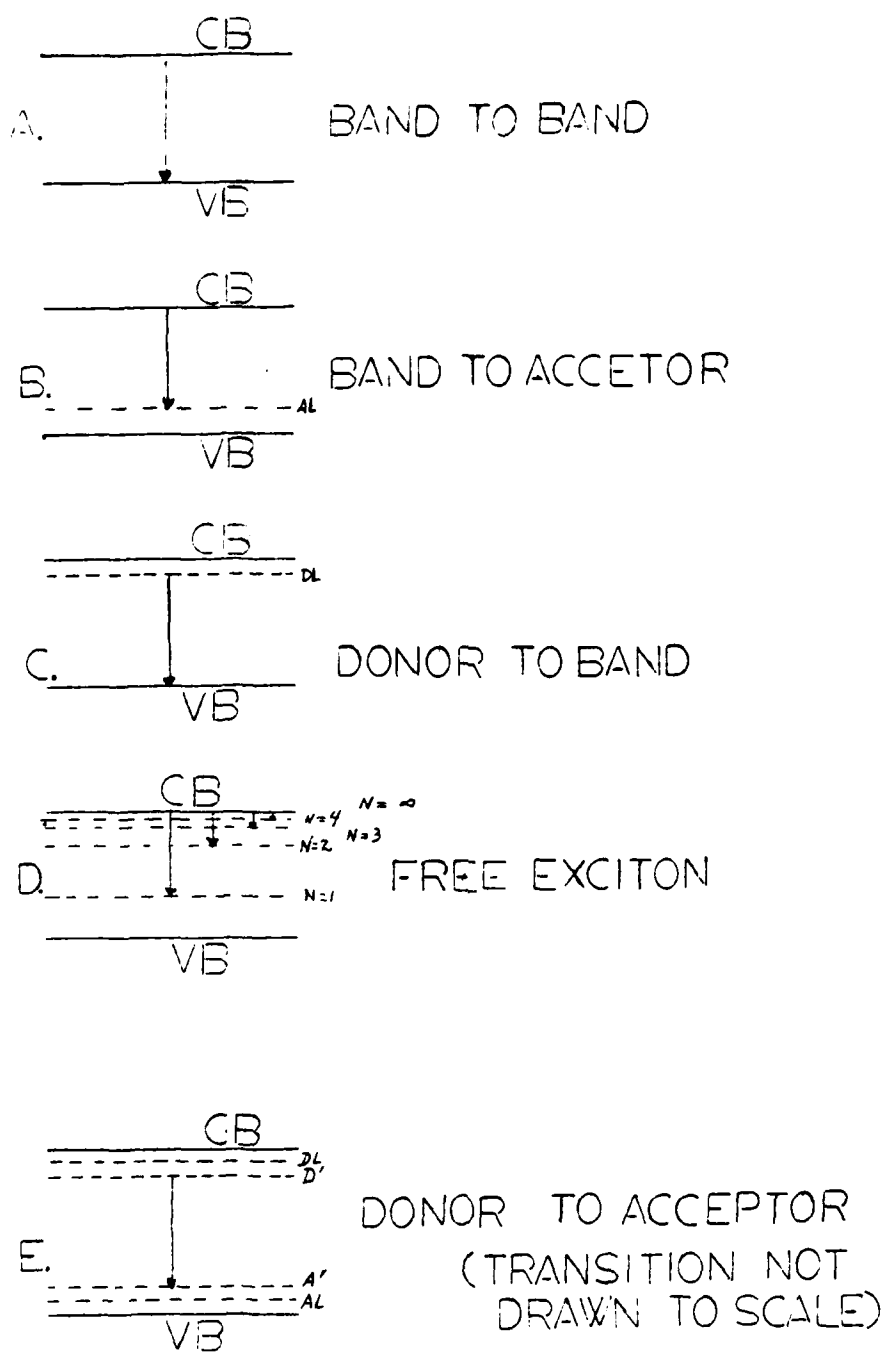


Fig. 2-1. Optical Transitions

can orbit the hole as if this were a hydrogen-like atom; this is called an exciton. The ionization energy is then²,

$$E_i = - \frac{m_r^* e^4}{2 \hbar^2 \epsilon^2} \frac{1}{n^2}$$

where n is an integer ≥ 1 indicating the various exciton states, m_r^* is the reduced mass,

$$\frac{1}{m_r^*} = \frac{1}{m_e^*} + \frac{1}{m_h^*} \quad , \quad \text{and } \epsilon \text{ the dielectric constant.}$$

The exciton, in this case, can wander through the crystal, hence it is called a free exciton. The electron and hole are now only relatively free because they are associated as a mobile pair. At high doping levels in the semiconductor local fields can exert a force on the electron and hole separately to cause the exciton to dissociate. High temperatures can also generate sufficient thermal energy to break the weak coulombic force of attraction that binds the exciton. Because of these facts, excitons are formed easily only in the purest materials and at low temperatures, even though exciton states represent the lowest energy states for EHP's³. When exciton emission is observed, the energy of emission differs from (B-B) recombination by the coulombic attractive energy which is often very small, since it is reduced by a factor m^*/ϵ^2 .

Donor-acceptor pairs can act as stationary molecules embedded in the host crystal. The coulomb interaction

between a donor and an acceptor results in a lowering of their binding energies. As a neutral donor and acceptor are brought closer together, the donor's electron becomes increasingly shared by the acceptor; they become more ionized. The amount by which the impurity levels are shifted due to the pairing interaction is simply the coulomb interaction inside a medium of dielectric constant, ϵ :

$$\Delta E = \frac{e^2}{\epsilon r}.$$

In a (D-A) pair, the energy of emission is

$$E_{D,A} = E_g - (E_D + E_A) + \frac{e^2}{\epsilon r}$$

where E_D and E_A are the respective ionization energies for isolated impurities.

B. History

The use of PL for the study of GaAs can be traced back almost two decades. The discovery of the injection laser in 1962 was particularly significant and the development of GaAs microwave devices and light-emitting diodes was a further stimulus to those studying the properties of this III-V semiconducting compound. The result of this interest was an enormous increase in the number of scientific papers published on GaAs; among these have been numerous studies of the luminescent properties of GaAs. Early work was hampered by the unknown quality of the crystals; good

theories concerning the cause of spectral lines seen in PL were scarce. Identification of these spectra was difficult due to a lack of knowledge of unwanted impurities often found in the crystal along with the desired substitutional impurities. More recent works in the PL study of GaAs have benefitted immensely from the ability of the semiconductor industry to grow crystals of high purity. Nathan and Burns in 1963 identified what they thought were (B-B) recombination and the $n = 1$ exciton in "pure" crystals of GaAs⁴. What they had actually seen were (B-A) and (D-B) transitions due to unknown and unwanted impurities introduced during crystal growth.

Along with crystals of questionable quality, early researchers were forced to use high intensity arc lamps to cause sample excitation; they found it necessary to filter this incoming radiation so that the output spectrum was not affected by anomalous emissions. Current PL research is greatly aided by the use of improved detector devices, much lower temperatures for sample observation, and very high purity crystals. These three facts have enabled researchers to identify the most common impurities introduced during crystal growth: Carbon (C), Copper (Cu), Si, and lattice vacancies and defects. Photomultiplier tubes and solid state detectors are both sensitive and accurate.

Lower temperatures (1° to 10°K) allow the researcher to identify transitions and states in the forbidden energy gap that have been hidden because the thermal energy of the lattice was too high. Pure crystals allow precise identifications of impurities to be made. The advent of the laser has solved the problem of finding a steady, high intensity source of excitation.

C. A Brief Look at Theory

PL, in terms of Quantum Electrodynamics, deals with the interaction between the radiation field and the atomic system and requires quantization of the radiation field in order to explain the absorption of energy and the promotion of electrons (and holes) to higher energy states'. Because I am studying the emission spectra of substrates, I am more interested in describing the emission process where optical radiation of characteristic energies from the sample can be identified between the bands.

Theoretical research concerning emissions and optical transitions in GaAs was introduced in the late 1950's by D. M. Eagles when he studied the transition between acceptor levels and the conduction band⁵. In 1963, W.P. Dumke, of I.B.M., published a quantum mechanical study which attempted to predict emission probabilities among bands and impurity levels and describe these in terms of carrier lifetimes in

GaAs . Assuming a direct energy gap between parabolic bands with the impurities taken to be shallow, discrete, and non-overlapping, Dumke calculates the maximum transition probabilities for:

a) donor to valence band (D-B) transition probability at $\vec{k}=0$:

$$\frac{1}{\tau_p} = 64 \sqrt{2} \pi n \frac{e^2 \hbar^2 \omega |P_{cv}|^2}{C^3 m^2 (m_c E_D)^{3/2}} n_D ;$$

b) conduction band to acceptor (B-A) transition probability at $\vec{k}=0$:

$$\frac{1}{\tau_n} = 64 \sqrt{2} \pi n \frac{e^2 \hbar^2 \omega |P_{cv}|^2}{C^3 m^2 (m_a E_A)^{3/2}} p_A ;$$

c) band to band (B-B) transition probability:

$$\frac{1}{\tau_m} = \frac{16 \pi e^2 \omega}{C^3 m^2 \hbar} |P_{cv}|^2 = \frac{16 \pi E_0 e^2}{C^3 m^2 \hbar} |P_{cv}|^2$$

where $|P_{cv}|$ is the averaged interband matrix element of the momentum operator; E_D and E_A are the impurity ionization energies; n_D and p_A are the concentrations (per unit volume) of electrons in donors, and of holes in acceptors, respectively; ω is the frequency that the impurity emits at; m_c is the mass of the electron in the conduction band; and m_a , an equivalent effective mass for acceptors, is 5 to 10 times greater than m_c . τ is the carrier lifetime. Higher energy carriers (at $\vec{k}=0$) have a lower transition probability.

According to Dumke, when electrons recombine from a Boltzman distribution, the carrier lifetime τ is dependent on temperature and carrier concentration. He uses the

lifetime to describe approximate transition probabilities; the longer the lifetime, the less likely is a transition. The less time that a carrier spends in either the conduction or valence bands, the more transitions will occur and the more intense will be the emission. The greater the impurity density, the greater is the probability for an optical transition because the lifetime is less. You cannot, however, decrease the lifetime by arbitrarily increasing the impurity concentration. At some point, impurity wave functions will begin to overlap and this will modify the wave functions of the impurities so that the effective mass theory of simple donors and acceptors will not be applicable. With a small amount of overlap, the impurity wave functions will have approximately the same envelope wave functions and calculated lifetimes will be almost correct.

CHAPTER III

This chapter details the mechanics of data taking and sample preparation. I will first describe my apparatus and how PL emission spectra are recorded. Following this I will present the surface preparation and encapsulation processes. Surface preparation of samples is normally not required for PL; it is done in this case to assure good adhesion of the film to the substrate. I discuss the encapsulation technique because it is relatively new; neutralized ion beam sputter-deposition has only recently been applied to depositing thin films. Since it does not require high temperatures, we may not see the same damage that other encapsulation processes generate.

A. PL Apparatus and Data Taking Procedures

Procedurally, the PL process and apparatus is relatively straightforward. As has been mentioned, no special sample preparation is necessary for PL. Some sample surfaces were cleaned prior to film deposition in order that impurities and imperfections at the surface be eliminated so that the deposited Si_3N_4 film would adhere to the substrate; this is normally not required for PL. The wafer to be examined must only be small enough to fit onto the cold finger of the dewar ($\sim 1\text{cm}^2$) but large enough to focus a laser beam on ($\sim 0.1\text{ mm}^2$). It is mounted on the cold finger of a Janis Cryogenic Dewar (see Fig 3-1) using a high thermal

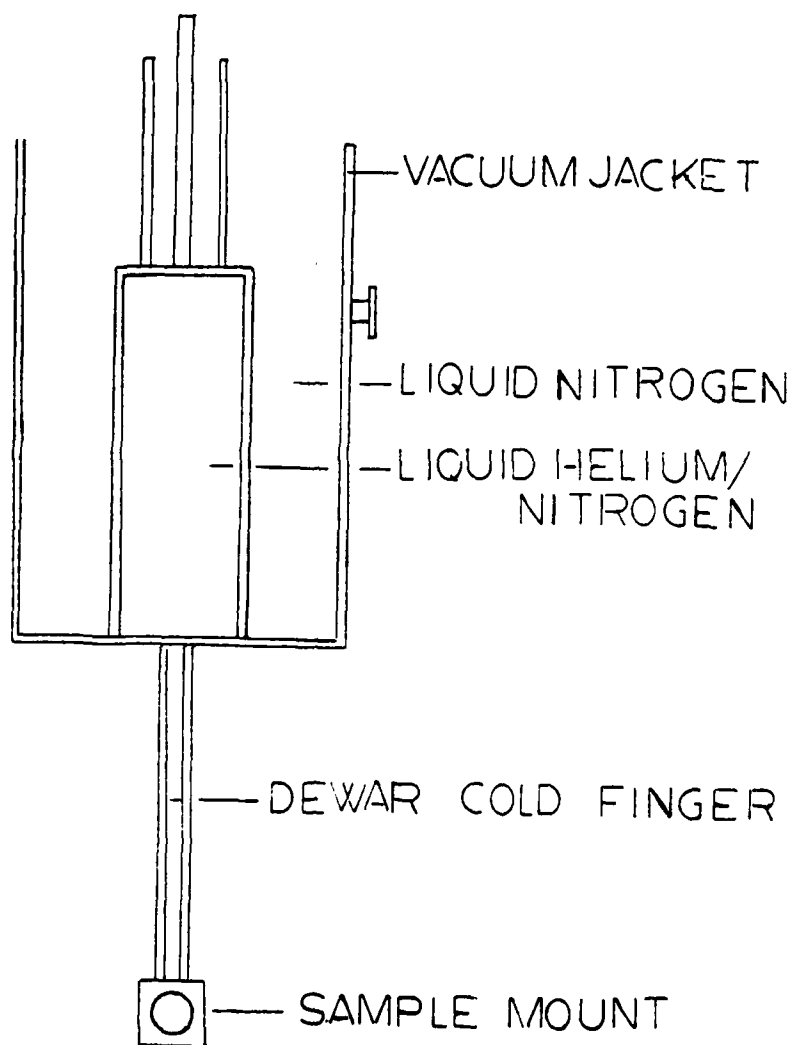
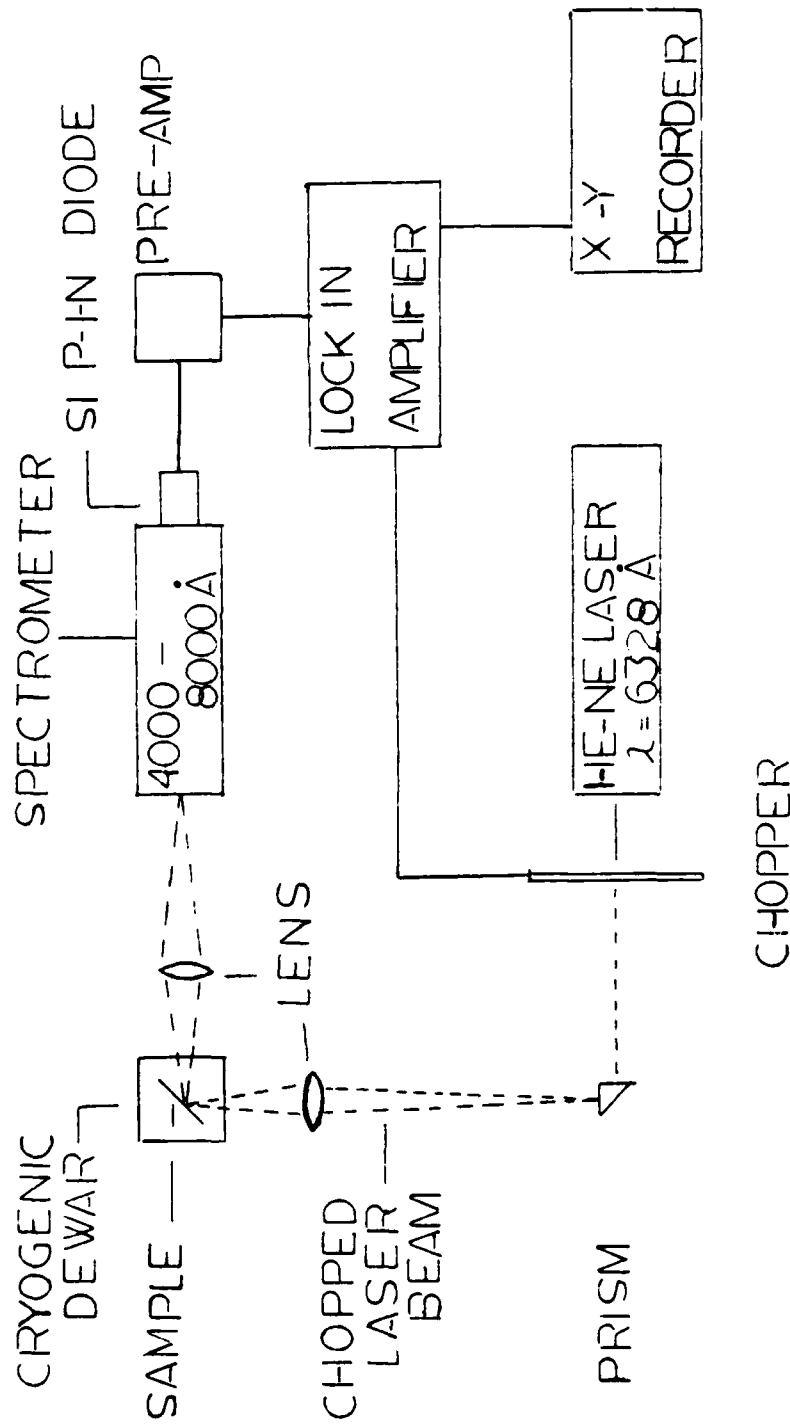


Fig. 3-1. Janis Cryogenic Dewar

conductivity paste to secure it in place. The dewar is then closed and attached to a vacuum system for pumpdown; this is done so that the dewar may later be cooled to very low temperatures without water vapor and other gaseous components condensing and freezing on the surface of the sample and to thermally insulate low temperature parts. The system is "roughed down" to 15 microns pressure and then opened to a diffusion pump for evacuation to the range of 10^{-6} to 10^{-7} TORR. The dewar is usually left connected to the vacuum pump for three to four hours to allow outgassing of the dewar, heat sink compound, and other components. After removal from the vacuum system, the dewar is filled with either liquid Nitrogen for PL at 77°K or liquid Nitrogen and liquid Helium for PL at 20°K. The dewar is then mounted and allowed to cool for ~30 minutes. After all electrical components have been operating for a sufficient amount of time to allow for accurate, steady readings, an emission peak is found and the signal is maximized by adjusting dewar position.

As seen in Fig (3-2) the beam from a 35 milli-watt (mW) Spectra-Physics 125 Helium-Neon (He-Ne) laser ($\lambda = 6328 \text{ \AA}$, $E = 1.96 \text{ eV}$) is focused on the sample through a quartz window in the tail section of the dewar, after being chopped by a 35 hertz (hz) mechanical shutter. The beam is chopped to provide a

Fig. 3-2. Photoluminescence apparatus

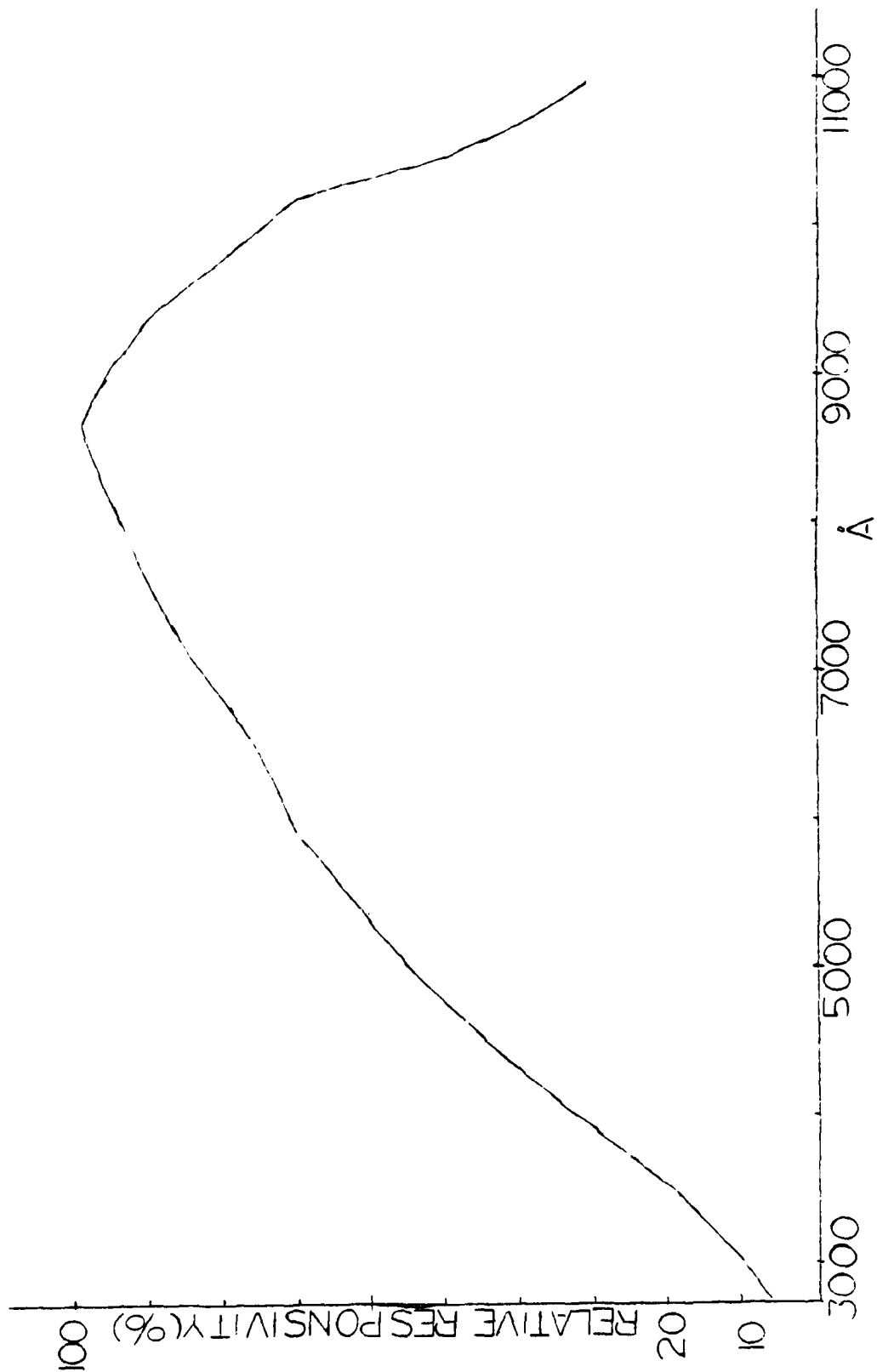


reference for a lock-in amplifier. When the light strikes the sample, EHP's are created. After a certain lifetime, τ , they recombine giving up photons of characteristic energies; these energies can be identified as transitions among bands and impurity levels. This recombination radiation passes through another quartz window in the dewar tail and is focused onto the entrance slit of a 1/2 meter Jarrell-Ash Scanning Spectrometer. Inside, this light is focused by a parabolic mirror onto a precision ruled grating which can be turned at varying speeds to present discrete, but relatively weak, wavelengths to the output slit as a function of time. At this output slit, optically sealed from other light, is placed a Si p-i-n detector, purchased from United Detector Technologies. Its sensitivity is greatest for optical radiation in the region from 6000Å to 10,000Å: below 6000Å, the dropoff is approximately linear; above 10,000Å, the dropoff is quite severe due to the band gap of Si. The sensitivity is shown in Fig (3-3).

A p-i-n detector is a p-n junction with a doping profile tailored in such a way that an intrinsic "i-region" is sandwiched between a "p-layer" and an "n-layer". Because of the low doping profile, most of the potential drop will occur across the intrinsic region. Absorption of light here produces EHP's; pairs produced in this region

Fig. 3-3. Relative spectral response of Si p-i-n diode

Fig. 3-3. Relative spectral response of Si p-i-n diode



PRECEDING PAGE BLANK-NOT FILMED

and within a diffusion length of it will eventually be separated by the electric field, leading to a current flow in the external circuit as carriers drift across the depletion region.

The current signal is taken from the detector to the input of a pre-amplifier where it is converted to a voltage signal. The voltage is then put into a PAR HR-8 Lock-in Amplifier. We have already provided a reference input of 35 hz from the chopper to the lock-in. The weak signal from the detector is modulated at 35 hz and the lock-in will distinguish this weak signal from the background noise. The lock-in detects only that portion of the incoming voltage that is both modulated at 35 hz and is in phase with the reference signal. A voltage output is provided from the lock-in to an x-y recorder where our spectra can be recorded.

B. Sample Preparation and Encapsulation

A stringent chemical cleaning procedure for the GaAs substrates was necessary to assure clean and reproducible surfaces for good adhesion¹⁰. Encapsulation was performed using neutralized ion beam sputter-deposition, a relatively recent technique for depositing thin insulator films⁸. In conventional sputtering, a target or cathode is eroded by the impact of energetic atoms from a plasma; the eroded

surface forms a vapor which then deposits on the walls, fixtures, and substrate. Neutralized ion beam sputter-deposition is accomplished using a 2.5 cm Kaufman-type ion source manufactured by Ion Tech, Inc., of Fort Collins, Colorado. The ion gun is mounted in a vacuum system and is shown in Fig (3-4). Argon (Ar) is used as the sputtering agent and is introduced directly into the ion source discharge chamber. When film deposition is desired, Nitrogen (N) is introduced in the vicinity of the substrate and the partial pressures of Ar and N in the 10^{-4} TORR range, although they can be made an order of magnitude lower. The ion source and beam current are adequately described in references eight and nine. Film deposition occurs when the neutralized Ar^+ ion beam sputters the Si target; Si atoms are ejected into the bell jar atmosphere and those near the GaAs substrate may combine reactively with N to cause the Si_3N_4 film to deposit. Because Oxygen (O) remains as a residual impurity due to the outgassing of components, it will also combine reactively with N and Si to form silicon oxy-nitride ($Si_3O_2N_4$). Exact film thickness and refractive index are determined using a Gaertner Research Ellipsometer. All substrates studied were deposited for ~30 minutes and varying thicknesses from 600Å to 850Å were obtained. Annealing was done in a quartz tube surrounded by resistive

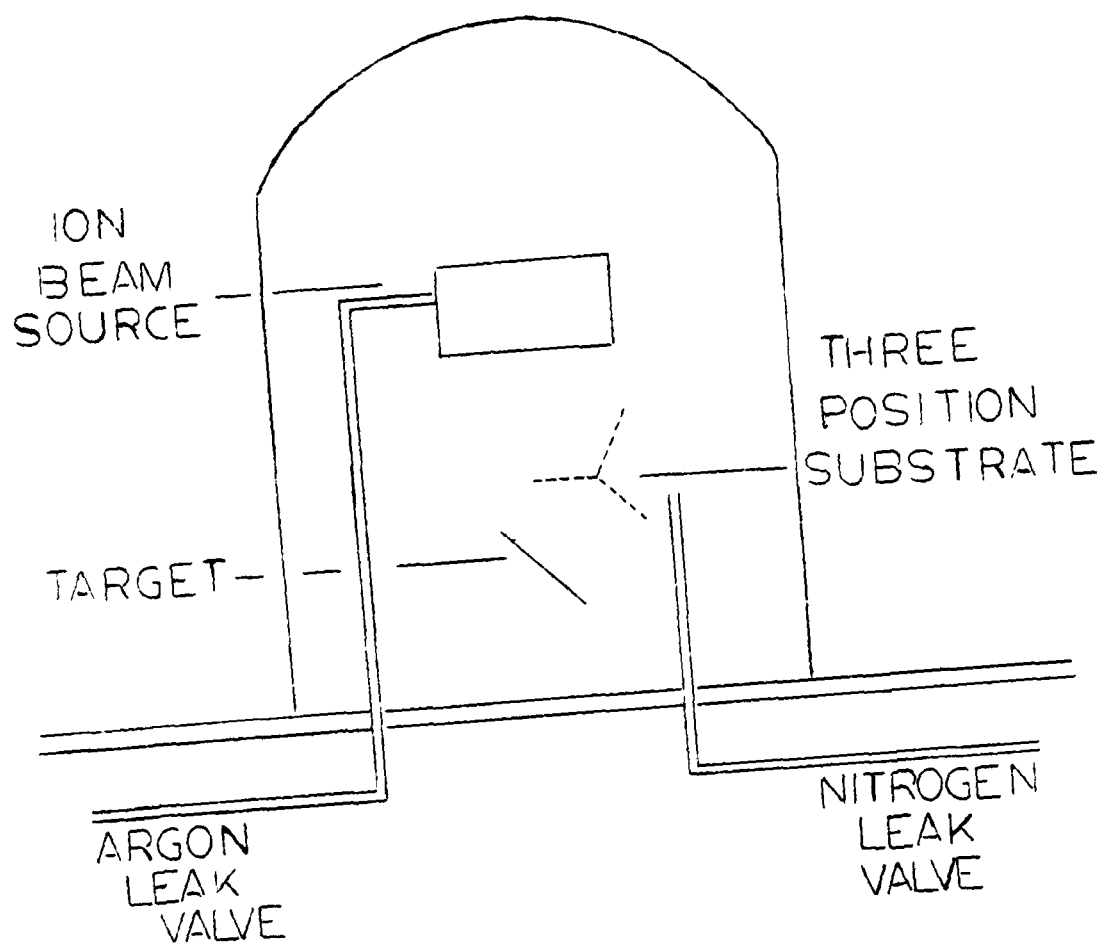


Fig. 3-4. Neutralized ion beam sputter-deposition apparatus
from J. R. Sites, Thin Solid Films⁶

heating coils and samples were flushed with ultra-pure Hydrogen (H) for 45 minutes at temperatures between 600°C and 950°C. Measurements were made of the ability of the film to resist high temperatures without degrading.¹⁰

Film composition was determined by trial and error, varying the partial pressure of N. Too low a partial pressure resulted in films which were very high in Si content as measured by the refractive index. As the partial pressure of N was increased, the film became more stoichiometric. When the refractive index began to saturate around 2.03, the film was primarily Si₃N₄ (with some O impurity). The saturation of the refractive index usually occurred when $pN_2 > 4 \cdot 10^{-4}$ TORR¹⁰. Films prepared as described and deposited in a properly pumped and degassed system showed refractive indices in the neighborhood of 2.03, good adhesion to the substrate, and good resistance to annealing with only etch pits observed in Si₃N₄ (Si₃O₂N₂) films up to 900°C.

Neutralized ion beam sputter deposition generally shows several advantages⁸:

- 1) independent control of beam current, beam energy, and film composition;
- 2) electrical neutrality of target and substrate because the Ar⁺ ion beam has been neutralized by the addition of free electrons;

- 3) relatively low energy collimated beam;
- 4) ability to sputter clean both the target and substrate, in situ, by rotating the sample holder;
- 5) relatively low bell jar pressure;
- 6) ease of reactive sputtering;
- 7) low temperature of film deposition;

Two drawbacks generally mentioned are the slow deposition rate and complex source. These disadvantages, however, are overshadowed by the favorable features listed, particularly the low temperature of deposition.

As can be seen, our main concern is with the emission of recombination radiation, its detection, and interpretation. We need only be concerned with the excitation in that we need a source providing photons with an energy greater than the band gap energy of GaAs and one that will provide high intensity light but not introduce anomalous emissions into our recorded spectra. The thrust of my presentation of theory was in emission and optical transitions and how these can be used in our investigations. The next chapter will attempt to interpret the data that we collected.

CHAPTER IV

Chapter four represents the heart of this thesis. In it, I will present the data that I gathered and use information from other research sources to analyze emissions that I see. I will proceed in three steps. First, I will discuss the PL spectra of bare, unannealed substrates. Next, I will give a short background on encapsulation and annealing and why it is necessary to distinguish what each process does to the substrate; then, I will describe papers from two different research groups who attempt to explain how annealing causes damage to the crystal. Finally, I will present my own observations on film deposition using neutralized ion beam sputtering and subsequent annealing of the GaAs substrate. From this, I will draw conclusions which will be presented in the last chapter.

A. Bare Substrate Analysis

As we see in Table I, the series "J" samples are moderately doped with Tellurium (Te), a group six (Gp VI) element. Te will enter the As sublattice as a substitutional donor (Te_{As}). It has six valence electrons: five satisfy the tetrahedral bonding of the As atom that it replaces and one is left which is easily ionized ($E_c \sim 3 \text{ meV}$) for conduction. This electron orbit is approximated by using a scaled hydrogenic orbit of radius

TABLE I: GaAs Wafer Information

Series	J	L	N
Vendor	Morgan	Morgan	Monsanto
Orientation	100	100	100
Dopant	Te	Te	Si
Concentration (cm^{-3})	$1.26 \cdot 10^{17}$	$5.13 \cdot 10^{17}$	$3.2 \cdot 10^{18}$
Mobility ($\text{cm}^2/\text{V}\cdot\text{sec}$)	1903	—	1664
Resistivity ($\text{ohm}\cdot\text{cm}$)	0.0358	0.00418	0.0012

$$a_p = \epsilon a_0 / m_c^*$$

where $a_0 = 0.53 \cdot 10^{-10}$ cm is the radius of the first Bohr orbit, ϵ is the dielectric constant, and m_c^* is the conduction band effective mass.⁷

Sample J-1 is a bare, unannealed substrate and Fig (4-1) displays its PL spectrum done at 20°K. The horizontal axis represents increasing wavelength in Angstrom units (Å) or decreasing energy in electron-volts (eV). The vertical axis indirectly represents emission intensity; it is a direct measure of the voltage output of the lock-in amplifier and the vertical units are largely arbitrary. All other spectra will be presented in this manner.

Three emissions are prominent in this spectrum: A at 8175Å (1.519eV), B at 8290Å (1.498eV), and C at 8510Å (1.459eV). We also observe a very broad weak emission at approximately ~10,000Å (1.23eV). The energy of the emission is calculated from:

$$E(\text{eV}) = \frac{hc}{e\lambda} = \frac{6.63 \cdot 10^{-34} \text{ J sec} \cdot 2.9979 \cdot 10^8 \text{ m sec}^{-1}}{1.6 \cdot 10^{-19} \text{ J (eV)}^{-1} \cdot \lambda(\text{m}) \cdot 10^{10} \text{ Å m}^{-1}} = \frac{12400}{\lambda(\text{Å})} \text{ eV}$$

Since peak A apparently falls ~2 meV below the value for E_g (20°K) as shown in Fig (4-2), it is assumed not to be a (B-B) transition. Several researchers have suggested that this emission is caused by free exciton recombination.¹¹ The 2 meV difference in energy, E_g (20°K) - 1.519eV, would then be due to the coulombic attraction experienced by the electron and hole after they form the exciton. The emission

Fig. 4-1. Sample J-1

SAMPLE J-1

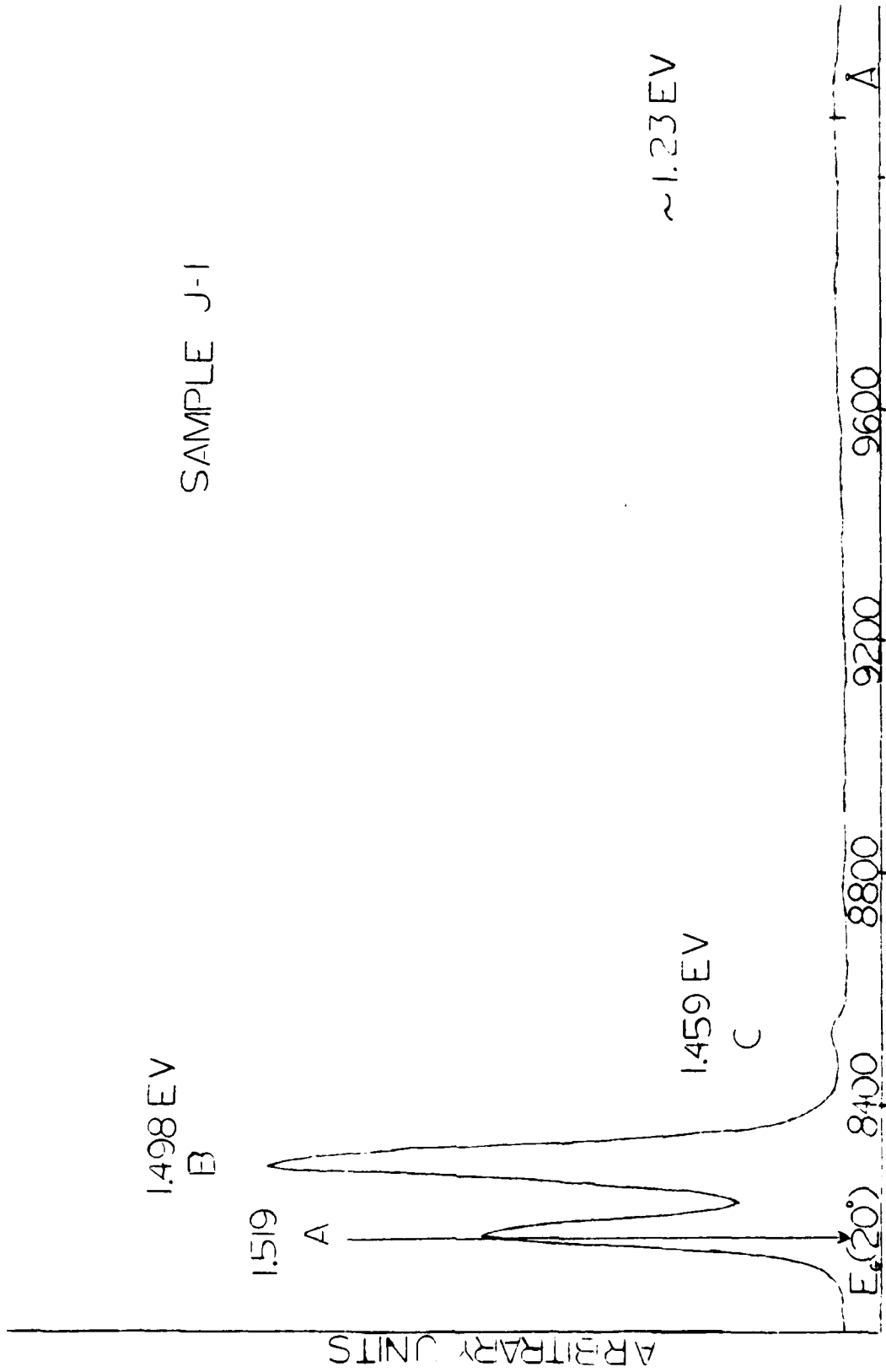
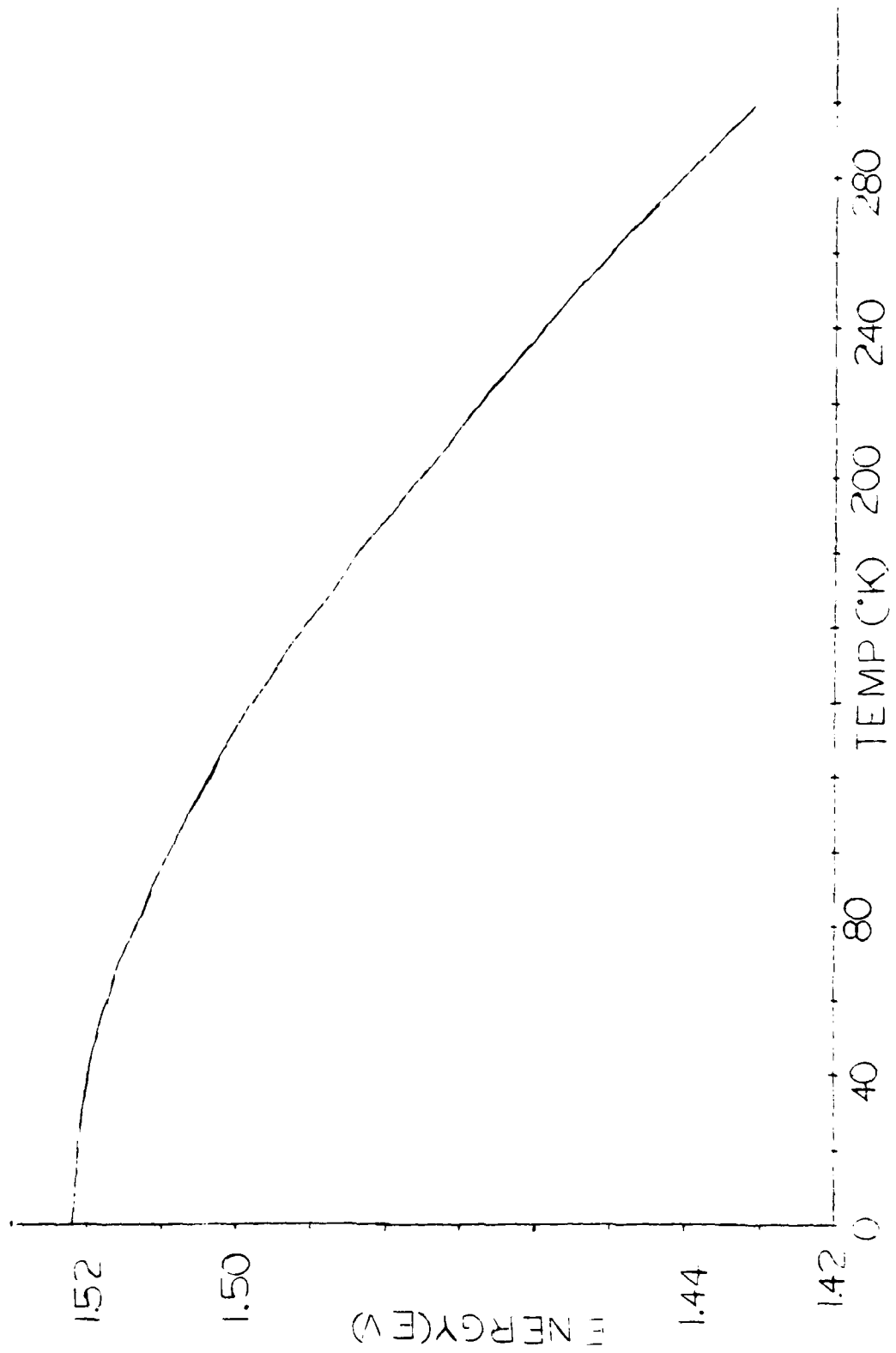


Fig. 4-2. Variation of GaAs band gap energy with temperature



PRECEDING PAGE BLANK-NOT FILMED

energy of 1.519eV would be due to the energy given up by the particles as they form the exciton. I previously mentioned, though, that excitons are usually formed only in the purest materials and at the lowest temperatures³. Driscoll, et al, tend to rule out exciton recombination because strong quenching of exciton associated luminescence begins to occur at 10°K.¹²

As an alternative, Driscoll, et al, attribute an emission in this energy range to a (D-B) transition caused by a simple, hydrogenic donor.¹² Since the primary dopant is Te_{As} then this transition would be from the Te_{As} donor level to the valence band. As evidence, they offer the fact that as the As content in the melt from which the crystal was pulled is increased, the emission half-width of a peak at 1.519eV decreases. As the As content is increased, the number of available sites for Te atoms to reside is decreased because the As vacancy (V_{As}) concentration decreases. Pankove has shown that the half-width profile of a hydrogenic defect is a sensitive function of the concentration of centers responsible for the peak, since it reflects the broadening of the impurity level into a band as the impurity concentration increases¹³. Changing the impurity concentration changes the emission half-width directly. Since our peak falls at the same energy, I attribute peak A at 8175Å (1.519eV) to be due to a (D-B)

transition. We may also be seeing some exciton and (B-B) recombination in this peak also, but the temperature is not low enough to resolve these as separate transition.

Emission B at 8290\AA (1.498eV) falls $\sim 24\text{ meV}$ below E_g (20°K). In this region are usually seen emissions caused by simple hydrogenic acceptor impurities. The ionization energy for acceptors is greater because the valence band effective mass is greater than conduction band effective mass and is governed by :

$$E_i = \frac{m_{\star}^* e^4}{2\hbar^2 \epsilon^2 m^2} = \frac{m_{\star}^*}{m \epsilon^2 m^2} 13.6 \text{ eV}$$

where n is a quantum number greater than or equal to one and 13.6eV is the ionization energy for the $n=1$ electron of the Bohr hydrogen atom. I assume that this is not due to Te_{As} donors since we have already identified peak A with them. Driscoll, et al, identify emissions in this region with simple hydrogenic acceptors in crystals grown close to stoichiometry. Again, when the As concentration in the melt increases, the emission half-width decreases. This implies, since V_{As} are decreasing, that emission B is due to an acceptor residing on an As site. As with the donor, the emission half-width is a sensitive function of impurity concentration¹³. Since Group IV atoms are acceptors on As sites in GaAs, Driscoll, et al, suggests either Carbon (C)

or Si as an unwanted impurity introduced into the lattice during crystal growth. A group from the Royal Radar Establishment in England has been able to identify numerous simple acceptors in GaAs by selective doping with particular impurities.¹⁴ Their results are shown in Table II. They have identified an emission at 26 meV below E_g (20°K) as being due to a C_{As} acceptor and attribute this peak to a transition between the conduction band and an acceptor level. This process will ionize the acceptor and depletes the conduction band of electrons to some extent. This C_{As} acceptor compensates the n-type substrate. Peak B has also been identified by a Japanese team as a (B-A) emission due to C_{As} .¹⁵

C is an unwanted impurity here, probably introduced during crystal growth. C is amphoteric, that is, it can be either a donor or acceptor depending on the conditions of growth and on which site it resides. C_{As} leaves an open bond; when it accepts an electron in this bond, it could be said that a hole is given up for conduction. In either case, the electron concentration of an n-type substrate is decreased by the presence of C_{As} .

Emission C in Fig (4-1) is a small peak at 8510 Å (1.459 eV). It falls ~39 meV below the C_{As} (B-A) transition and can be identified as a longitudinal optical (LO) phonon replica of the C_{As} emission. The value of 39 meV

TABLE II: Energies of Spectral Lines in GaAs

Acceptor	Observed (B-A) Transition (5 K, eV \pm 0.3meV)	Binding Energy (meV) (Ground State)
Carbon (C)	1.4935	26.0
Silicon (Si)	1.4850	34.5
Germanium (Ge)	1.4790	40.4
Tin (Sn)	1.349	171
Zinc (Zn)	1.488	30.7
Cadmium (Cd)	1.4848	34.7
Beryllium (Be)	1.4915	28.0
Magnesium (Mg)	1.4911	28.4

is only slightly above the measured value of 36 meV for the energy of the LO phonon in GaAs. A phonon replica peak results from a phonon assisted optical transition. These transitions, which in general have a reduced probability, occur when the impurity atoms are strongly coupled to the GaAs. The reduced possibility is evident in the intensity of the phonon replica emission: it is much less than the C_{AS} emission. The energy of the optical portion of the phonon replica can be given by

$$E_{PR} = (E_G - E_A) - b E_P$$

where E_P is the energy of the LO phonon and b is the number of phonons emitted. In our case, $b = 1$, and, in general, emission with $b > 1$ is very weak. Since $E(C_{AS}) - E(PR) \approx 39 \text{ meV}$ the frequency of the emitted phonon would be

$$\omega = \frac{E}{\hbar} = \frac{3.9 \cdot 10^{-2} \text{ eV} \cdot 1.6 \cdot 10^{-19} \text{ J (eV)}^{-1}}{1.0546 \cdot 10^{-34} \text{ J sec}} = 5.9 \cdot 10^{13} \text{ sec}^{-1}$$

The very wide emission at $\sim 10,000 \text{ \AA}$ ($\sim 1.23 \text{ eV}$) has been seen by numerous researchers^{12, 17-22}. Several facts are common to this emission. It is usually seen only in crystals grown close to stoichiometry. It is not seen in p-type substrates or crystals grown from Gallium (Ga) rich melts; both of these would tend to suppress Ga vacancies (V_{GA}). The emission is seen only in GaAs doped n-type with Gp-IV or Gp-VI impurities. These facts imply the presence of V_{GA} and donors as a cause for this emission. Williams has

suggested that this ~1.2eV band is due to a complex center of (V_{CA} -GpIV $_{CA}$) or (V_{CA} - GpVI $_{AS}$). Since we already have Te_{AS} , a GpVI atom as the known impurity, I will assume that the complex is (V_{CA} - Te_{AS}). The V_{CA} acts as an acceptor and the Te_{AS} acts as a donor.

Assume that the Te_{AS} donor absorbs sufficient energy to free the sixth electron: the V_{CA} then accepts this electron. A coulombic force now exists between the Te_{AS}^+ and the V_{CA}^- and according to Williams' configuration-coordinate model in Fig (4-3), the complex is not in equilibrium and in coming closer because of the attraction to a new equilibrium position, the lattice emits a phonon.¹⁷ Later, the V_{CA}^- gives up the electron to the Te_{AS}^+ donor and the complex will emit a photon of energy

$$E_{(V_{CA}-Te_{AS})} = E_0 - (E_A + E_D) + e^2/\epsilon r.$$

After this photon has been emitted and the complex is neutral again, the components are closer than their neutral equilibrium positions and they relax back to these positions emitting a phonon. The complex is again ready for excitation. We can represent the energy process by :

$$E_{ABS} - E_{PHONON} = E_{EMS} + E_{PHONON}$$

This is also called a Stoke's Shift. While no direct evidence exists for a configuration-coordinate model of the (V_{CA} - Te_{AS}) emission, Williams implies that this theory is correct because Hwang has identified a similar occurrence

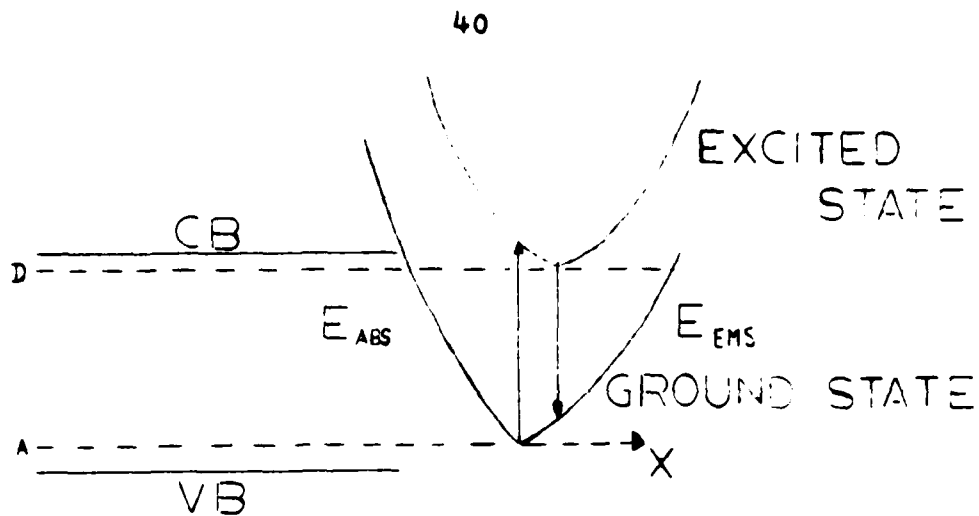


Fig. 4-3. Williams' configuration-coordinate model from Physical Review¹⁹

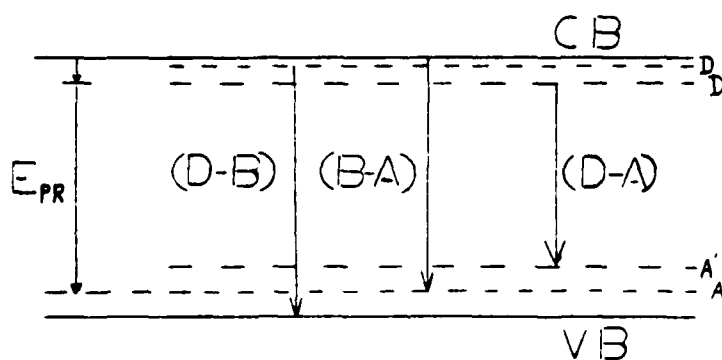


Fig. 4-4. Summary of transitions, Sample J-1

in GaAs for the (V_{As} - acceptor) complex.²³ Using Hwang's information, Williams has calculated the displacement of the lattice from equilibrium between neutral and excited states as being $5.33 \cdot 10^{-10}$ cm (0.0533\AA).²⁴

Several Soviet researchers have offered an alternative explanation which involves a Te donor complexed with an interstitial atom, presumably Oxygen (O).²⁰ Here O atoms occupy interstitial positions and are thus labeled O_i . They act as acceptors and when they acquire an electron from a Te_{As} , they become coulombically attracted to the Te_{As} donor and form a complex. The Russians are able to explain some structure seen in this emission in terms of which vacant tetrahedron the O_i^- occupies so that the distance between the components of the complex is different. This changes the attraction and causes emissions of two different energies. They offer as proof the fact that the emission is seen to intensify after ion implantation of Oxygen. This interstitial model is weakened considerably, however, because it neglects the rather gross lattice distortions that would occur if the oxygen was, in fact, interstitially located.

Neither theory gives an entirely satisfactory explanation of this broad emission at $\sim 10,000\text{\AA}$; neither presents definite proof. The important fact to remember is that this emission probably represents an interaction between an

impurity and either a native defect or another impurity. The O_i^- or V_{Ga} will act as acceptors along with the C_{As} to compensate the crystal. These acceptors act as traps to deplete the conduction band and donor level of electrons.

As a short review, I believe that PL allows us to identify the known dopant, Te_{As} , through a (D-B) transition. A (B-A) emission shows us that an unwanted acceptor impurity, C_{As} , is present. We also see some complex formation involving the known donor, Te_{As} , and an acceptor, either V_{Ga} or O_i^- . The net effect of these acceptors is to decrease the electron concentration by providing traps; it compensates the crystal. We also observe a LO phonon replica of the C_{As} (B-A) emission which is the result of strong lattice coupling. These are seen in Fig.(4-4).

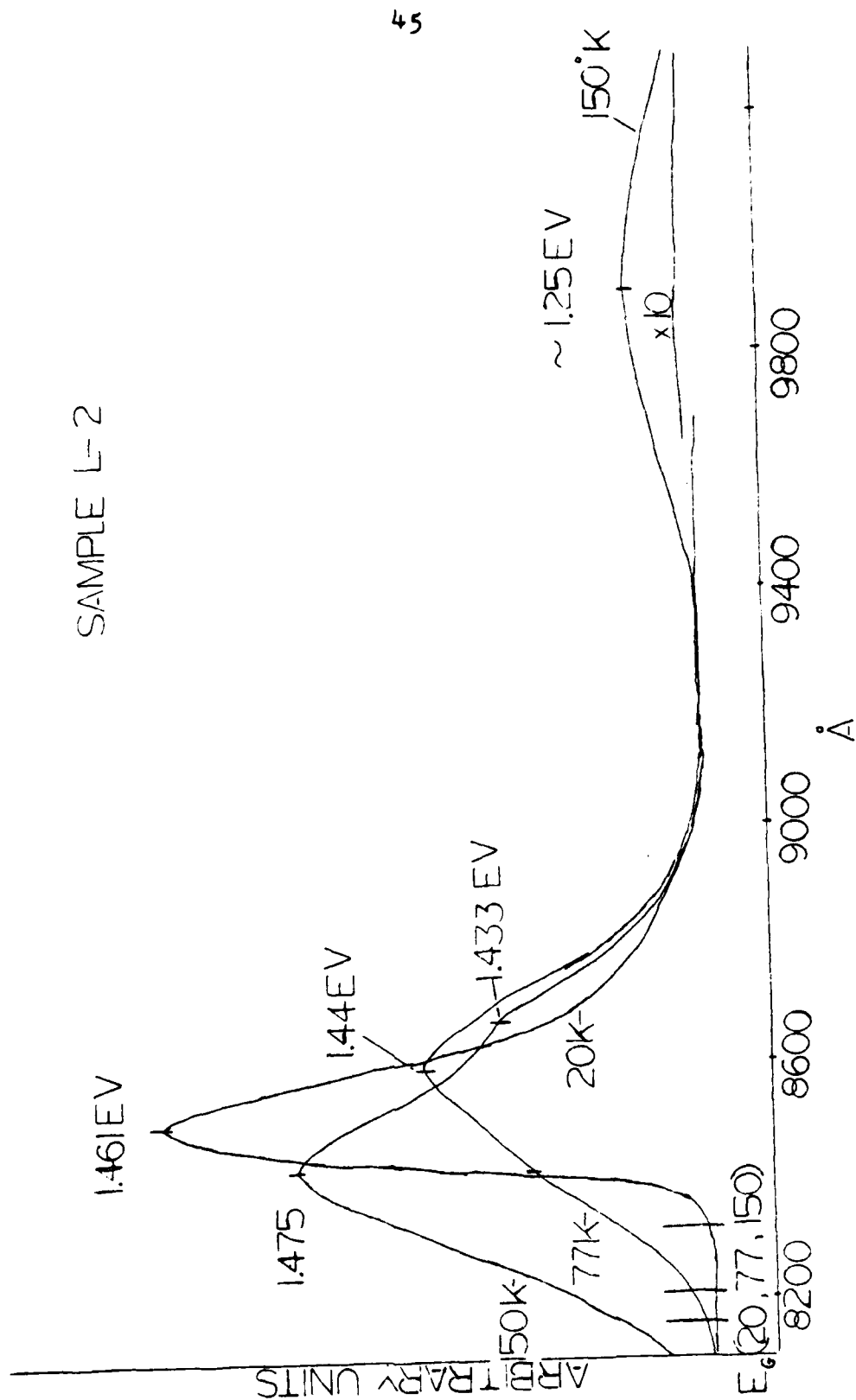
When the substitutional impurity or its doping level is changed, the PL spectra is changed. Generally, the ionization energies of the impurities are different so that if we change the impurity, we will see transitions of varying energies as in Table II. As we increase the impurity concentration, we decrease the average distance between impurities until their wave functions begin to overlap. When this happens, the effective mass approximation for simple donors and acceptors can no longer be used.⁷ As a result of this increased concentration, the emission half-width

increases and adjacent emission peaks begin to run together. This causes apparent shifts in the emission energies that we see. Impurity levels begin to broaden and will merge with the nearest intrinsic band when their density is large enough. When we have more than one impurity present and the distance between these impurities is decreased sufficiently, donor-acceptor pairs and complexes begin to form. These interact coulombically sharing an electron.

The "L" series samples have Te_{As} donors ($n_D = 5.13 \cdot 10^{17} \text{cm}^{-3}$) and the PL spectra of sample L-2 are shown in Fig (4-5) at three different temperatures. At 150°K, we see a large emission at 1.475eV with a lower energy shoulder at 1.433eV. In accordance with Kressel, et al, I attribute the 1.475eV emission to (B-B) recombination with the 1.433eV emission too indistinct to identify.²⁵ At 77°K, we see the main emission at 1.44eV with a high energy shoulder at 1.475eV. Kressel, et al, investigated GaAs doped with both Si_{As} and Te_{As} and they attributed a peak at ~1.44eV to a Si_{As} acceptor or a complex involving Si acceptors, possibly ($\text{Si}_{\text{As}} - \text{V}_{\text{As}}$)^{12,23,25}. They grew their crystal from a Ga rich melt that would suppress V_{As} and enhance V_{As} , causing Si_{As} and V_{As} . From these facts, I believe that the 77°K, ~1.44eV emission may be due to some type of Si acceptor; this is not definite, but since the curves are so similar I believe that

Fig. 4-5. Sample L-2

SAMPLE L-2



Si is present. This implies the existence of Si as an unwanted impurity. The high energy shoulder at 1.475eV is probably due (B-B) recombination. At 20°K, we see a single emission at 1.461eV which is probably due to Si acceptors or a complex involving Si acceptors, shifted to a higher energy because of the lower temperature of observation.

At higher temperature (~150°K), the (B-B) transition dominates because Si and Te donors are ionized, providing numerous carriers to the bands for recombination. At 77°K the holes are "frozen" at acceptor sites, so that the (B-A) emission at ~1.44eV dominates; we still may have some holes in the valence band which may cause the (B-B) recombination that we see in the high energy shoulder but the valence band is largely depleted. At 20°K, apparently all holes are frozen at acceptor sites and we are seeing only the (B-A) emission involving Si_{As} acceptors or a complex involving Si_{As} acceptors. The unwanted Si acceptor dominates the spectra and even though we have a large concentration of Te_{As} donors, we see no direct evidence of them.

Fig (4-6) shows the PL spectra at 20°K of a heavily doped n-type substrate of GaAs: Si ($N_D = 3.2 \cdot 10^{18} \text{ cm}^{-3}$) with only one broad emission at ~8150Å (~1.521eV) which is essentially a (B-B) transition. This substrate is so heavily doped that the half-width of the peak is very broad.

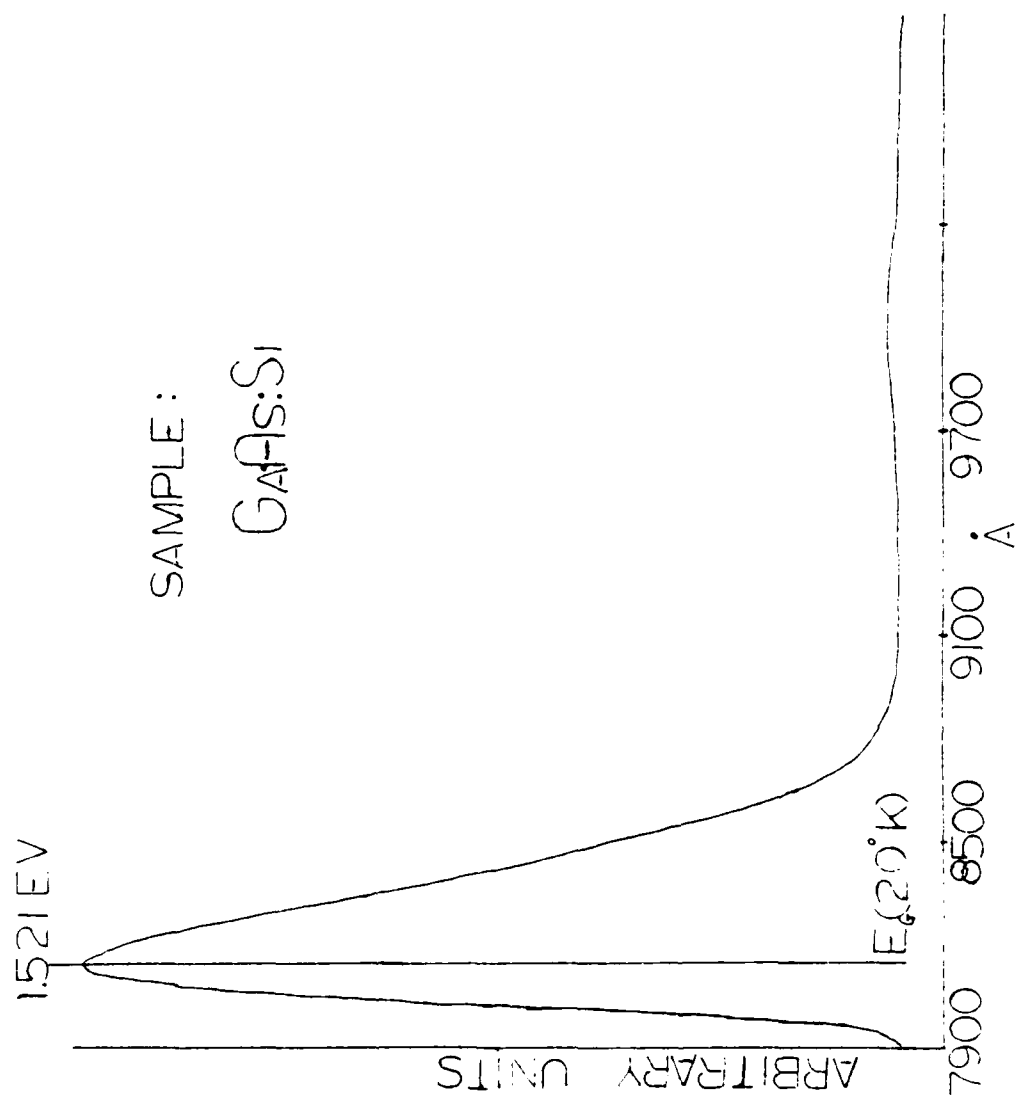


Fig. 4-6. Sample GaAs: Si

Si is a shallow donor in GaAs when situated on a Ga site and because of the high impurity concentration, the Si donor level has probably merged with the conduction band and the crystal is degenerate.

B. Encapsulation and Annealing

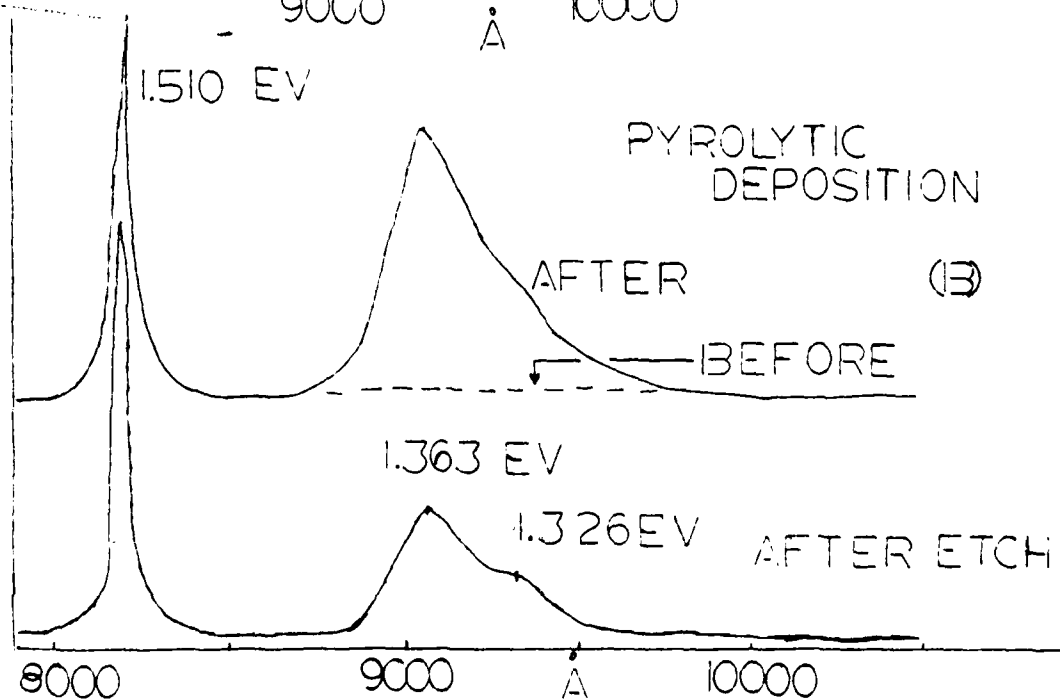
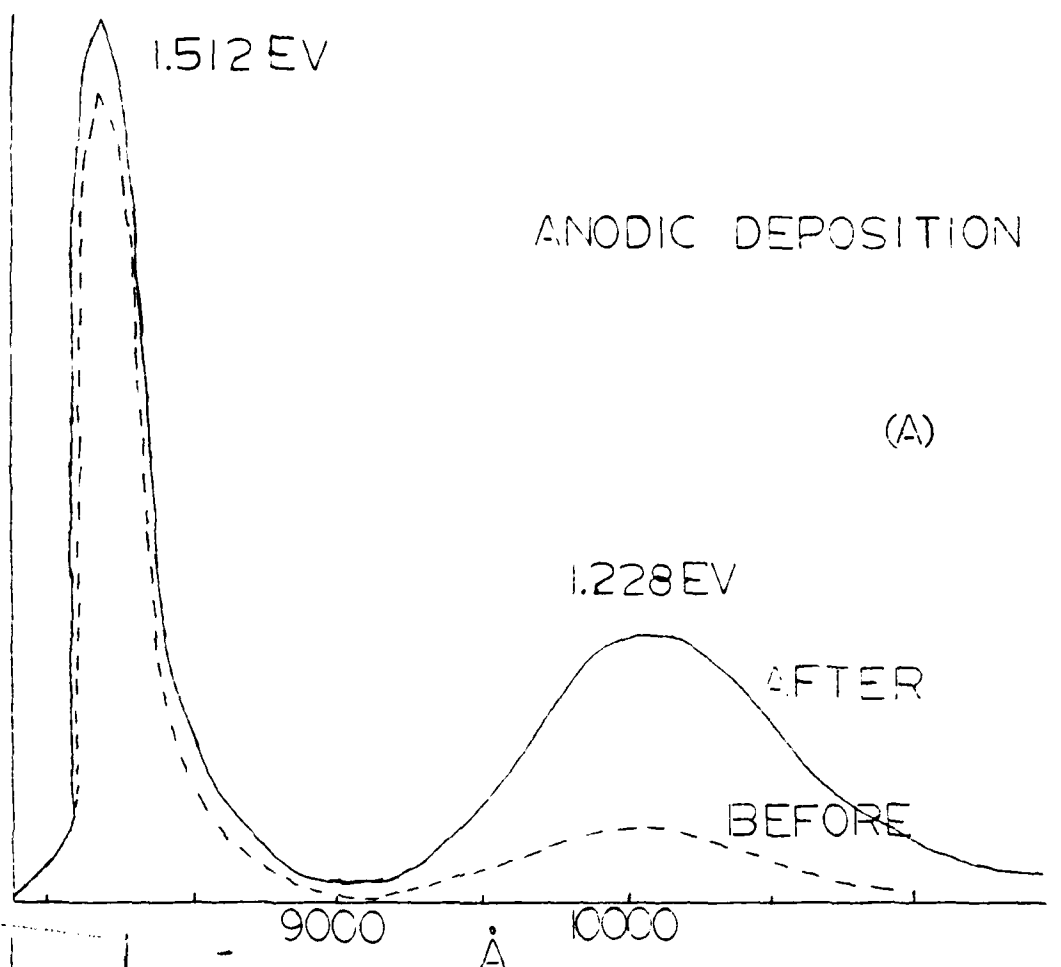
Encapsulation and annealing are two very important steps in the fabrication process of GaAs semiconducting devices. Encapsulation is the process by which a thin insulating film is deposited on a semiconducting substrate. It is done to prevent As out diffusion during ion implantation annealing. Annealing is a high temperature process that brings order to a crystal lattice which has been damaged during ion implantation or etching; it causes interstitial atoms to occupy electrically active sites.

A primary task of this thesis is to determine the effect of annealing on bare and deposited substrates. It has long been known that heat treatment causes serious damage to the crystal lattice of compound semiconductors. Since several methods of film deposition require an elevated substrate temperature, we first need to know if our encapsulation process causes defects to occur in the substrate. We must be able to distinguish deposition from annealing effects. Once we have separated these effects, we will observe annealed substrates and attempt to determine the composition of the defects and/or impurities and then try to discover the process that creates them.

Several methods of film deposition have been used. They generally differ in the temperature at which deposition takes place. Lum, et al, deposited dielectric films anodically and pyrolytically.¹⁷ Fig (4-7A) shows the 77°K PL spectra of a n-type GaAs: Si substrate on which has been deposited anodically a film of $\text{Si}_3\text{N}_4(\text{Si}_x\text{O}_y\text{N}_z)$. This process is done at room temperature and it is important to notice that no new emissions are seen after the deposition in comparison with the pre-deposition spectrum. On the other hand, when the $\text{Si}_3\text{N}_4(\text{Si}_x\text{O}_y\text{N}_z)$ film is pyrolytically deposited at 600°C, two new emission appears at 9130Å (1.36eV) and 9320Å (1.33eV) which did not occur in the bare substrate. These are presented in Fig (4-7b) and after etching the new peaks are suppressed. The peaks at 9120Å/9320Å are believed to be the same as defects caused during annealing. The defect creation process will be discussed in the next section and since neutralized ion beam sputter-deposition is done at room temperature, I may not see these heat related defects in our samples after deposition.

Because GaAs shows promise for use in high frequency applications, much research has been expanded to understand the processes which act on the crystal during annealing.^{17,27-36} Chatterjee, et al, from the University of Illinois, have annealed bare and deposited substrates of GaAs under varying conditions.²⁷ PL at 6°K of lightly doped ($\sim 10^{16} \text{ cm}^{-3}$) GaAs: Cr is shown in Fig (4-8, a-e). Fig (4-8a) shows a

Fig. 4-7. Si_3N_4 deposition techniques



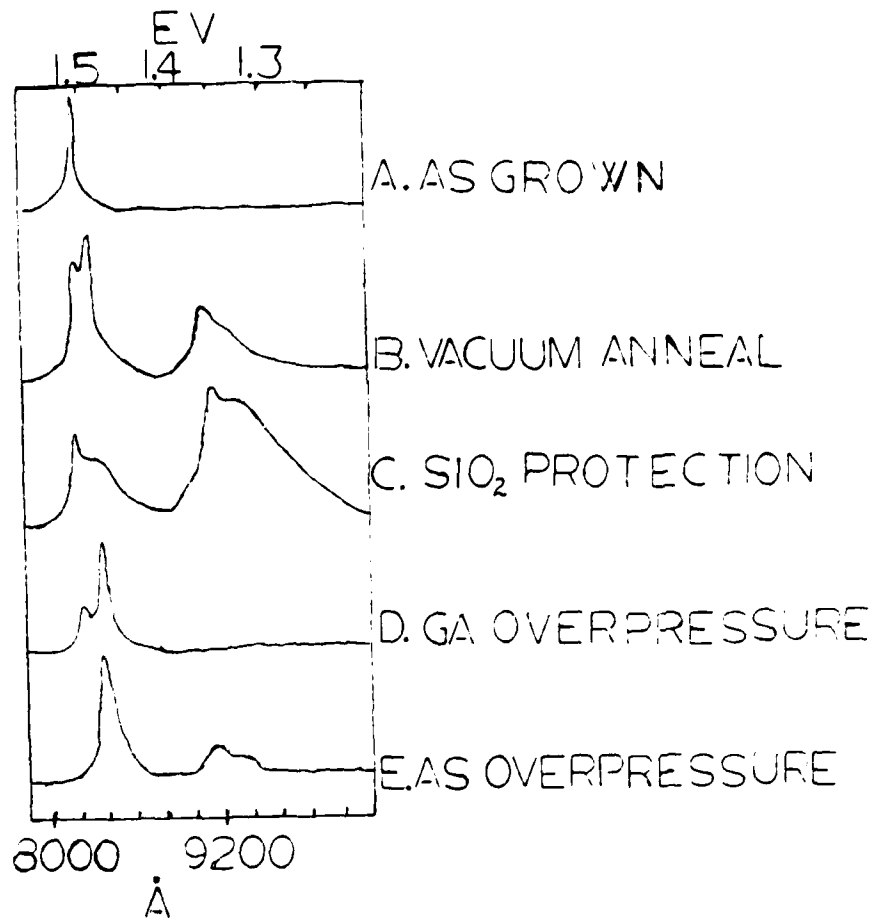


Fig. 4-8. PL spectra at 6 K from Chatterjee, et al, Solid State Communications²⁷

spectra of a bare, unannealed substrate and a single emission at 8170Å (1.52eV) is seen. This is attributed to (B-B) recombination. Fig (4-8b) is of a bare sample that has been annealed in an evacuated silica ampoule for one hour at 850°C. Several differences are immediately obvious. The intensity of the emissions has decreased; along with the 8170Å (1.52eV) peak, we also see peaks at 8340Å (1.49eV), 9120Å (1.36eV), and 9320Å (1.33eV). Fig (4-8c) shows the result of annealing a substrate capped with 2000Å of SiC₂ in a vacuum. The intensity of the 8340Å emission is suppressed slightly while the 9130Å (1.36eV) and 9320Å (1.33eV) peaks are enhanced. In Fig (4-8d) we see the results of an anneal done of a bare substrate done in a Ga overpressure; the 8340Å (1.49eV) peak is enhanced while the lower energy emissions are not observed. Fig (4-8e) details the change when a bare substrate is annealed in an As overpressure. Here, the 8340Å (1.49eV) peak is suppressed in comparison with Fig (4-8d) while the 9120Å (1.36eV) and 9320Å (1.33eV) peaks are present again.

The vapor pressure of As is significantly greater than that of Ga; therefore, upon annealing a bare substrate, we would expect to see large numbers of V_{As} generated at the surface. Encapsulation of GaAs is performed to suppress As out diffusion. When this is done, though, it has been found that the encapsulant allows, and sometimes encourages,

the out diffusion of Ga.^{36,38} In Fig's (4-8b-c) we see the 8340Å (1.49eV) peak more intense after the bare substrate has been annealed than after annealing with a cap. It is also obvious that the 9120Å (1.36eV)/9320Å (1.33eV) emissions are enhanced after annealing with a cap. On the basis of this information, the Illinois group assign the 8340Å (1.49eV) peak to V_{As} and the 9120Å (1.36eV)/9320Å (1.33eV) peaks to V_{Ga} . As additional proof, bare substrates annealed in a Ga overpressure show enhanced emissions at 8340Å (1.49eV). Ga overpressure would suppress V_{Ga} (the 9120Å/9320Å emissions) and enhance V_{As} (the 8340Å emission). This is observed. Annealing done in As overpressure should suppress V_{As} (8340Å emission) and enhance V_{Ga} (9120Å/9320Å emissions). This is also seen. The basic point of Chatterjee, et al, is that annealing (or heat treatment) will cause dissociation of GaAs at the surface. Depending on whether or not the substrate is covered, one species will preferentially leave. They claim that annealing causes vacancies only.

Lum, Wieder, and their associates at the Naval Ocean System Center interpret this process differently.¹⁷ In Fig (4-7b) they saw an emission at 9120Å (1.36eV)/9320Å (1.33eV) after the pyrolytic deposition of their dielectric film. If Chatterjee, et al, had done a PL spectra after the reactive deposition of their dielectric film at 440°C,

they may have seen the same emission that they attribute to annealing. This is why it is so important to be able to distinguish deposition and annealing effects. Lum, et al, believe the cause of these emissions to be a (V_{Ga} - Acceptor) complex where the acceptor might be Si_{As} . Annealing with a cap promotes V_{Ga} at the surface and these diffuse into the bulk. Excess Si atoms from dielectric film breakdown also diffuse in and occupy V_{As} ; these components then complex and cause the 9120\AA (1.36eV)/ 9320\AA (1.33eV) emissions. Kressel, et al, have seen an emission at 1.37eV which he attributes to a deep Si acceptor (Si_{As}) impurity or a complex involving Si acceptors,²⁵ so that it is possible that we are seeing a (V_{Ga} - Si_{As}) complex as the cause of the emission at 9120\AA (1.36eV)/ 9320\AA (1.33eV). Since the separation of these two emissions is approximately the energy value for the LO phonon in GaAs, the 9320\AA (1.33eV) emission is considered to be a phonon replica of the 9120\AA (1.36eV). The Illinois group do see these 9120\AA /9320Å emissions when bare substrates are annealed in As overpressures and this appears to support their theory that only V_{Ga} causes this emission since no Si seems to be present. However, all of their annealing was done in Silica ampoules so that Si could migrate into the substrates at high temperature to interact with the V_{Ga} .

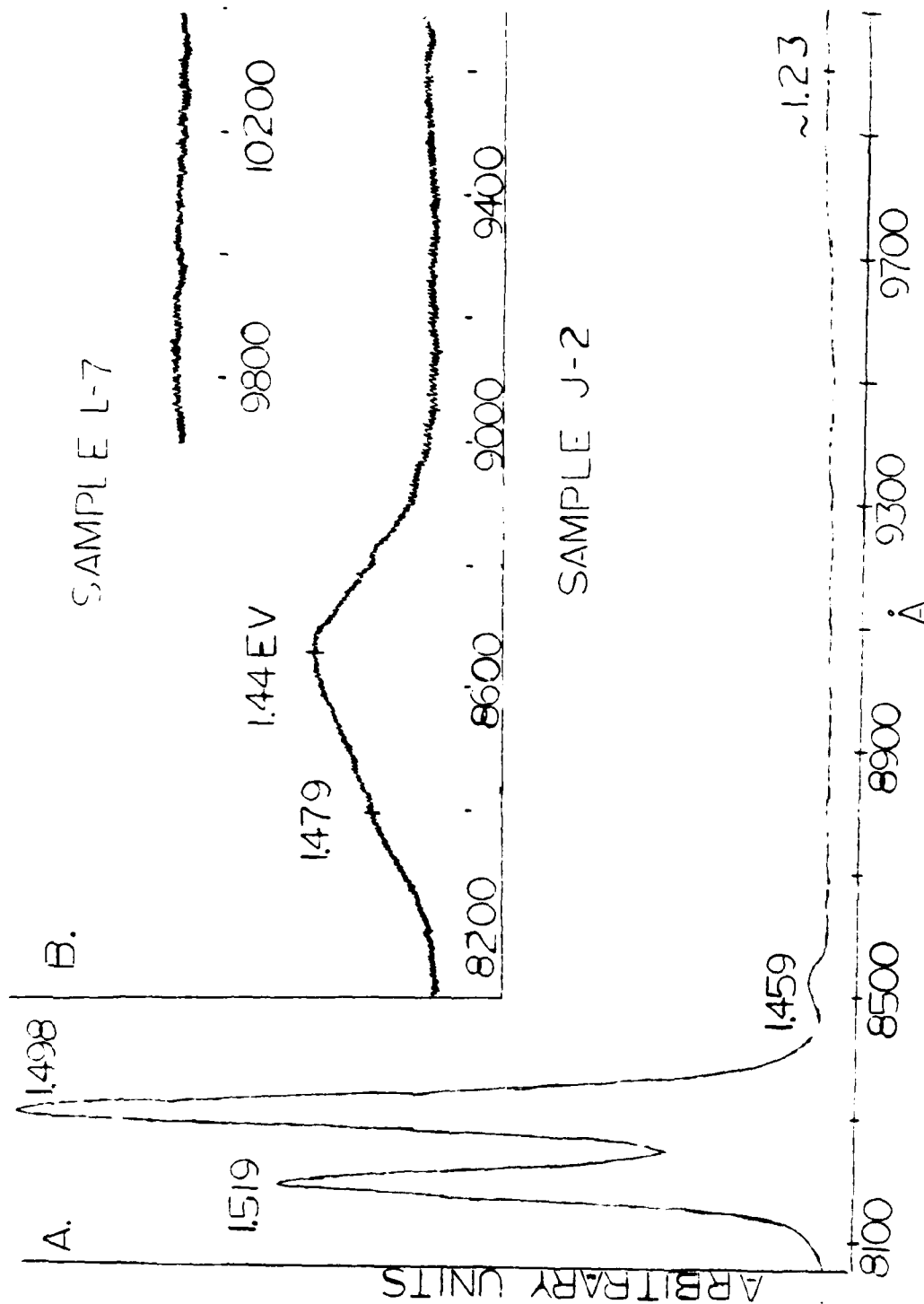
When the surface was etched by Lum, et al, they found that these annealing-related defects were suppressed and they finally disappeared after 154m of the surface was removed. This implies that the annealing only degrades the surface and not the entire substrate.

C. Observations on Encapsulation and Annealing

We have shown that any type of heat treatment will cause damage to the surface of the substrate. We have noted that dielectric film deposition will introduce annealing-like defects if the deposition temperature is high enough. Since it is absolutely necessary to distinguish the damage caused by deposition from that caused by annealing, we will study PL spectra of substrates sputter-deposited with $\text{Si}_3\text{N}_4(\text{Si}_x\text{O}_y\text{N}_z)$ to detect any type of deposition damage.

Sample J-2 shown in Fig (4-9a) was sputter-deposited with 850Å of $\text{Si}_3\text{N}_4(\text{Si}_x\text{O}_y\text{N}_z)$ as described in chapter three. The spectra was done at 20°K and shows no differences at all when compared to Fig (4-1) and sample J-1. Likewise, Fig (4-9b) is the 77°K PL spectrum of sample L-7 ($\text{GaAs: Te, } n_D = 5.13 \cdot 10^{17} \text{ cm}^{-3}$) sputter-deposited with 800Å of $\text{Si}_3\text{N}_4(\text{Si}_x\text{O}_y\text{N}_z)$; this, too, shows no changes when compared to the 77°K spectrum of Fig (4-5). Neither of these substrates showed any new emissions and peaks that were present in the bare substrate were not altered.

Fig. 4-9. Samples J-2, L-7

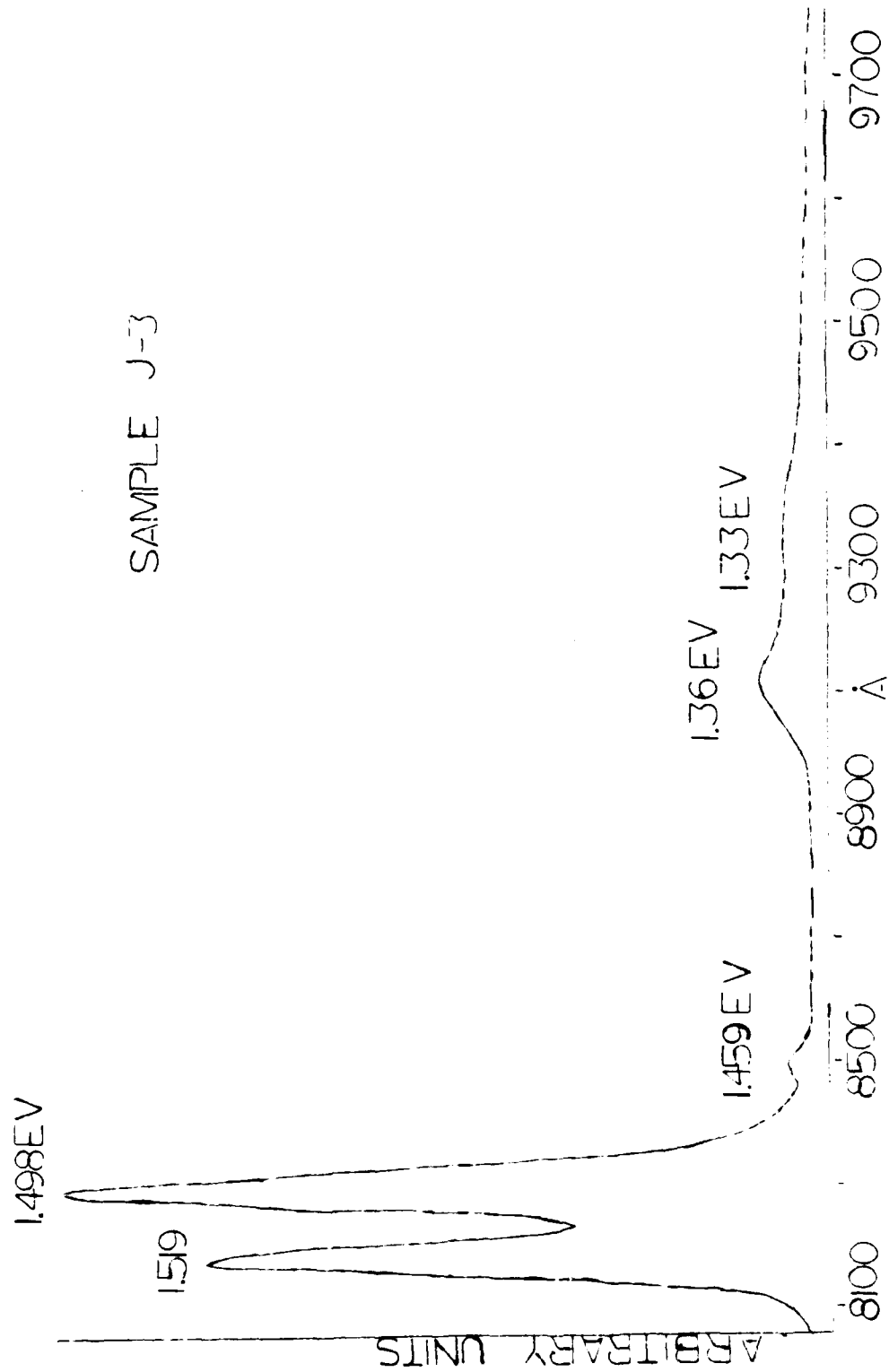


It is apparent that no new radiative transitions were introduced into the substrate by neutralized ion beam sputter-deposition at near band gap energies that we can detect. Since this method does not require high temperatures at the substrate for film deposition, it does not induce annealing related defects. Since we see no defects introduced during deposition, any damage detected after annealing encapsulated substrates can be attributed directly to the annealing.

We have discussed the effect that annealing has on GaAs. We assume that the annealing of encapsulated substrates causes a ($V_{Ga} - Si_{As}$) complex which forms near the surface of the substrate. The formation of this complex occurs when V_{Ga} are preferentially generated at the surface of encapsulated samples and diffuse into the bulk where they complex with Si atoms in-diffusing because of dielectric film breakdown.

Sample J-3 was sputter-deposited with 850\AA of Si_3N_4 ($Si_3O_4N_2$) and annealed in flowing H_2 gas at 750°C for 45 minutes. We previously noted that sputter-deposition did not cause annealing related damage so that any new emissions observed can be attributed directly to annealing. As shown in Fig (4-10), the three higher energy emissions remain unchanged; they were identified as a (D-E) transition

Fig. 4-10. Sample J-3



at 8175\AA (1.519eV) due to Te_{As} donors, a (B-A) transition at 8290\AA (1.498eV) due to C_{As} , and a LO phonon replica of the C_{As} (B-A) emission at 8510\AA (1.459eV). Two facts can be immediately observed. We see two new emissions at 9120\AA (1.36eV) and 9320\AA (1.33eV) and we apparently no longer see the broad, weak emission at $\sim 10,000\text{\AA}$ ($\sim 1.23\text{eV}$).

The emission at $\sim 10,000\text{\AA}$ ($\sim 1.23\text{eV}$) was previously attributed to a ($\text{V}_{\text{Ga}} - \text{Te}_{\text{As}}$) complex. It may be that the two new emissions simply mask the $\sim 10,000\text{\AA}$ ($\sim 1.23\text{eV}$) emission. Hwang has shown that the intensity of this ($\text{V}_{\text{Ga}} - \text{Te}_{\text{As}}$) complex increases after annealing.¹⁸ Since we are not seeing this, the new emission may be a more efficient trap than the ($\text{V}_{\text{Ga}} - \text{Te}_{\text{As}}$) complex. Since we are only observing a thin layer at the surface of the substrate, it may be that the cause of the new emission resides in the surface layer and is the dominant emission here in this energy range.

The emissions at 9120\AA (1.36eV) and 9320\AA (1.33eV) are identical with peaks at the same energy discussed by Chatterjee, et al,²⁷ and Lum, et al,¹¹ and seen in Fig's (4-7b and 4-8b,c, and e). We attributed these emissions to a ($\text{V}_{\text{Ga}} - \text{Si}_{\text{As}}$) complex and their formation was described previously. In moderately doped encapsulated samples, the formation depends on the creation of V_{Ga} , the addition of Si atoms from film breakdown, and the diffusion of both into the bulk.

This same annealing defect may also be present in two other n-type annealed substrates that we studied: GaAs : Te (L samples) and GaAs : Si (N samples). They can not be positively identified as the ($V_{Ga} - Si_{As}$) complex because they appear at slightly lower energy, as shown in Fig (4-11), at $\sim 1.32\text{eV}$ in sample L-3 and at $\sim 1.294\text{eV}$ in sample N-3. Both of these emissions, along with the $\sim 1.44\text{eV}$ emission in sample N-3, though, are annealing related since none existed prior to the annealing.

If we do assume that the $\sim 1.32\text{eV}$ and $\sim 1.294\text{eV}$ are caused by the ($V_{Ga} - Si_{As}$) complex, their shift in energy might be explained in several ways. Since these emissions are close to very large, broad emissions, it is possible that peaks affect each other and that we see a superposition that changes the energies slightly. When large numbers of impurities and defects are present, the lattice may be distorted so that the energies of transitions are modified. This is described by Quantum Defect Technique.³⁷ Finally, since the spectra in Fig (4-12) are done at 77°K and not 20°K , the increased temperature of observation will tend to broaden emissions and shift them to lower energy.

Since sample L-3 is unencapsulated, but may be showing the same ($V_{Ga} - Si_{As}$) defect emission that capped substrates show, another process must be at work. Annealing uncapped substrates usually produces V_{As} . Several researchers have noted that Si atoms transfer sites during annealing according

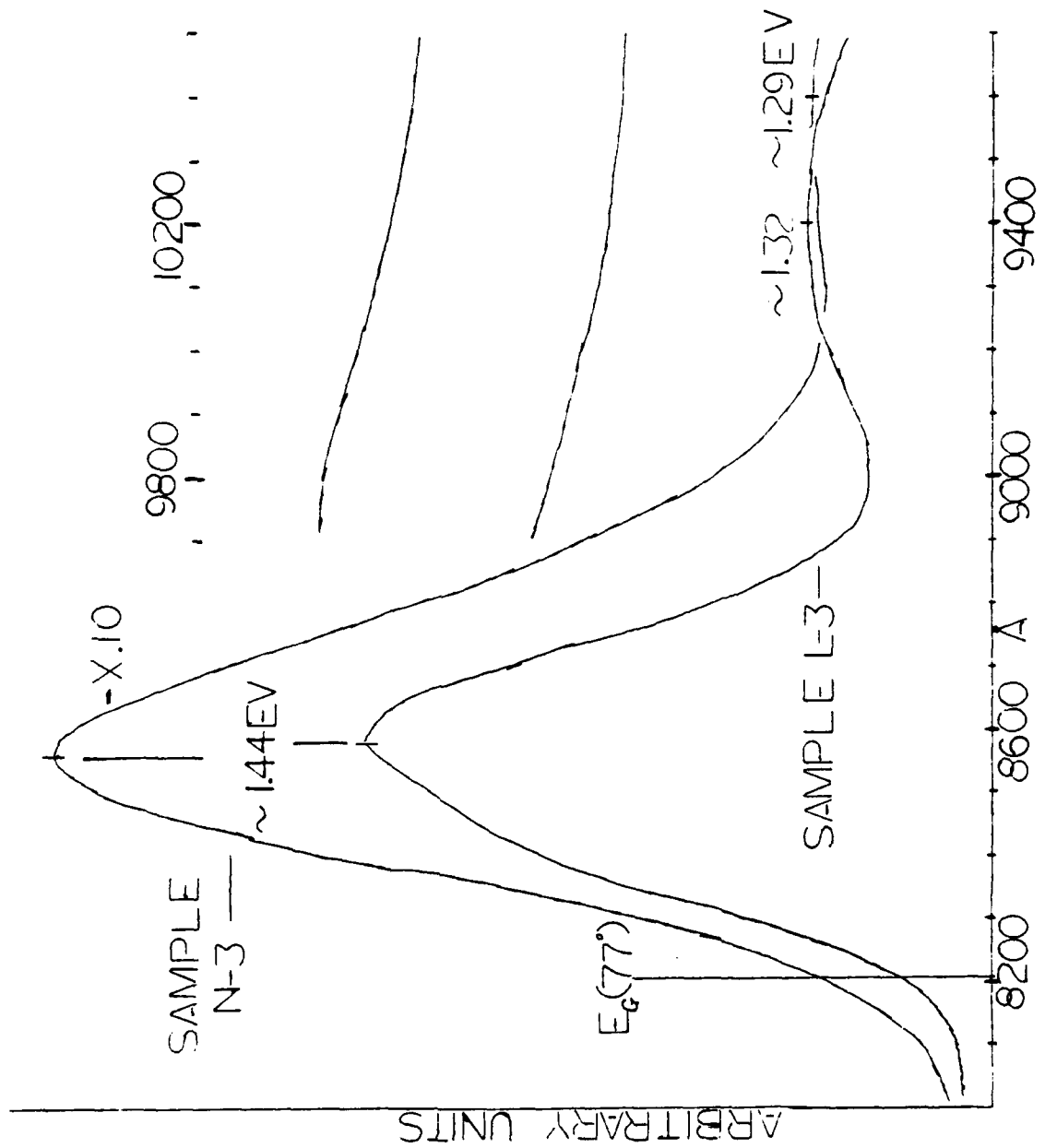
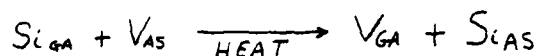


Fig. 4-11. Samples L-3, N-3

to the relation ^{11,34}:



and Lum and Wieder have seen the 9120Å/9320Å in annealed n-type GaAs: Si. Apparently in sample L-3, the 750°C annealing causes the generation of V_{As} at the surface and these diffuse into the substrate. When V_{As} become adjacent to Si_{Ga} , the site transfer takes place and we see the annealing complex ($\text{V}_{\text{Ga}} - \text{Si}_{\text{As}}$). We have already identified Si as an unwanted impurity in the "L" samples.

This same site transfer process may have occurred during the 935°C anneal of n-type GaAs: Si ($n_0 = 3.2 \cdot 10^{18} \text{ cm}^{-3}$) if we assume the emission at 1.294eV is due to ($\text{V}_{\text{Ga}} - \text{Si}_{\text{As}}$). The unannealed substrate from this crystal was shown in Fig (4-6) and we saw only a (B-B) transition so that the 1.44 eV emission in Fig (4-11) is also annealing related. It falls at approximately the same energy as the emission in "L" samples identified as a (B-A) transition caused by Si_{As} acceptors or a complex involving Si_{As} acceptors so that transfer of Si from Ga to As sites could have induced the 1.44eV emission. I should point out that all peak assignments in the heavily doped n-type GaAs: Si are hypothetical since the heavy doping makes positive identification almost impossible. We require V_{As} and Si_{Ga} for the site transfer process to create the ($\text{V}_{\text{Ga}} - \text{Si}_{\text{As}}$) complex along with temperatures greater than 700°C.

CHAPTER V

Conclusions

1.) PL spectra have shown the presence of unwanted impurities and defects in bare, unannealed n-type substrates along with the known substitutional impurities. These unwanted impurities were:

- a) C_{AS} resulting in a (B-A) transition in GaAs: Te, $n_p = 1.26 \cdot 10^{17} \text{ cm}^{-3}$;
- b) Si_{AS} resulting in a (B-A) transition or a band to Si_{AS} complex transition in GaAs: Te, $n_p = 5.13 \cdot 10^{17} \text{ cm}^{-3}$;
- c) V_{GA} resulting in a ($V_{GA} - Te_{AS}$) complex in GaAs: Te, $n_p = 1.26 \cdot 10^{17} \text{ cm}^{-3}$ and GaAs: Si, $n_p = 3.2 \cdot 10^{18} \text{ cm}^{-3}$.

In all cases, these impurities and defects are acceptors and tend to compensate the crystal.

2.) Neutralized ion beam sputter-deposition does not introduce radiative defects or impurities into the substrate during encapsulation. PL done of encapsulated samples showed no differences when compared to bare substrates. This was important because we can distinguish deposition and annealing effects. Defects that appear after annealing can be attributed directly to the annealing process.

3) Annealing encapsulated substrates will cause the formation of a vacancy-impurity defect that causes an emission at 9120\AA (1.36eV) with a phonon replica at 9320\AA (1.33eV) in the PL emission spectrum. I assume that this complex is

composed of ($V_{Ga} - Si_{As}$) in accordance with the theory of Lum, et al.^{11,17} The process of formation of this complex depends on the fact that V_{Ga} are generated in greater numbers than V_{As} in an encapsulated substrate during annealing; they form at the surface and diffuse into the bulk. Si atoms are freed from the film because of film breakdown at high temperatures and will also diffuse into the bulk. Here some Si will occupy V_{As} site and complex with V_{Ga} to form this complex.

The 9120\AA (1.36eV)/ 9320\AA (1.33eV) emissions have been seen by other researchers after film deposition¹⁷ and annealing.^{11,27} The lowest recorded temperature that caused the formation of this complex was 410°C . It is usually seen after heat treatment in the range of 600° to 800°C . The emission of this complex is easily seen in light to moderately doped samples where the impurities are sufficiently separated in the lattice so that the effective mass approximation can still be used for describing the impurity wave functions.

4.) In Fig (4-11) we may also be seeing this ($V_{Ga} - Si_{As}$) complex emission at 9400\AA (1.32eV) in the GaAs: Te ($n_0 = 5.13 \cdot 10^{17}\text{cm}^{-3}$) and at 9600\AA (1.294eV) in the GaAs: Si ($n_0 = 3.2 \cdot 10^{18}\text{cm}^{-3}$). The shift of this emission to lower energy might be explained in several ways. First, the spectra in Fig (4-11) were done at 77°K and the spectrum in Fig (4-10) was done at 20°K .

The increased temperature of observation will broaden the emission and usually shift it to lower energy. Second, as the impurity and defect concentration increases, wave functions begin to overlap; when this happens, the lattice may become distorted so that an apparent shift in emission energy has been observed. An attempt has been made to describe this perturbation using Quantum Defect Technique.³⁷ Third, as the emission half-widths broaden, peaks that are close to each other will begin to merge and the emission energies are changed by this superposition.

5.) If the emissions at 9400\AA in the "L" samples and 9600\AA in the "N" samples are due to $(V_{Ga} - Si_{As})$, then they and the 8600\AA (1.44eV) peak in the annealed "N" sample seen in Fig (4-11) are caused by site transfer of Si in GaAs. Si has been identified as an unwanted impurity in the "L" samples and is the primary dopant in the "N" samples. Annealing causes transfer of Si from Ga to As sites, leaving V_{Ga} and forming the components of the $(V_{Ga} - Si_{As})$ complex. Spitzer and Allred³⁸ and Lum and Wieder²² have identified this process; it requires Si_{Ga} and annealing temperatures greater than 700°C .

6.) The creation of this complex is assumed to take place only at the surface of the substrate. V_{Ga} are generated at the surface and diffuse into the bulk. Lum and Wieder²² found that this emission at $9120\text{\AA}/9320\text{\AA}$ would disappear

after $15\mu m$ were etched from the substrate. Chatterjee, et al, found the emission would disappear after only $.75\mu m$ were removed.²⁷

7.) This complex acts as an acceptor and its creation will compensate the surface of an n-type substrate. This effect is even more pronounced in semi-insulating GaAs where the surface will become p-type.

The heat treatment of n-type GaAs substrates will cause surface conversion in encapsulated substrates and apparently in Si doped unencapsulated substrates also. When growing epitaxial layers of n^+ GaAs on n^- GaAs or SI substrates at high temperature the introduction of a p-type interface in between is intolerable and interferes with the desired operation of any multi-layer device by introducing parasitic devices. Dielectric film deposition can introduce a parasitic p-n junction.

We must learn how to prevent this annealing damage or understand the process so that it can be exploited. It may be possible to produce Field Effect Transistors if this surface conversion due to the $(V_{Ga} - Si_{As})$ complex can be understood so that a controlled technique may be used to produce defect layers of desired characteristics. This thesis has been an attempt to examine how this complex affects the surface of n-type GaAs substrates.

BIBLIOGRAPHY

1. H. Bebb, E. Williams, Semiconductors and Semimetals, Vol. 8, Chaps. 4 and 5
2. R. S. Snow, Solid State Physics, Supplement 5, ed. Seitz, Turnbull, Academic Press (1957)
3. J. Pankove, Optical Processes in Semiconductors, Dover, 1971, Pg. 124
4. Nathan, Burns, Phys. Rev., 129, 125 (1963)
5. D. M. Eagles, J. Phys. Chem. Solids, 16, 76 (1960)
6. W. P. Dumke, Phys. Rev., 132, 1998 (1963)
7. W. Kohn, Solid State Physics, ed. Seitz, Turnbull, Academic Press, 1957, Vol 5, Pg 274
8. J. R. Sites, Thin Solid Films, 45, 47 (1977)
9. H. Kaufman, P. Reader, G. Isaacson, AIAA International Electric Propulsion Conference, Key Biscayne, Florida November 14-17, 1976
10. L. E. Bradley, J.R. Sites, to be published, J. Vac. Soc.
11. W. Y. Lum, H. Wieder, private communication
12. C. Driscoll, A. Willoughby, E. Williams, Journal of Materials Science, 9, 1615 (1974)
13. J. Pankove, J. Appl. Phys., 39, 5368 (1968)
14. D. J. Ashen, et al, J. Phys. Chem. Solids, 36,1041,(1975)
15. M. Ozeki, et al, Jap. J. Appl. Phys., 13, 1121 (1974)
16. Williams, Blacknall, Transactions of the Metallurgical Society of AIME, 239, 387 (1967)
17. W. Y. Lum, L. Messick, C.R. Zeisse, J. Appl. Phys., 49, 3602 (1978)
18. C. J. Hwang, J. Appl. Phys., 40, 4584 (1969)

19. E. W. Williams, Phys. Rev., 168, 922 (1967)
20. B. Kolesov, Z. Akkerman, L. Borisova, Sov. Phys. Semicond., 8, 425 (1974)
21. E. W. Williams, Brit. J. Appl. Phys., 18, 253, (1967)
22. H. Kressel, et al, J. Appl. Phys., 39, 5139 (1968)
23. C. J. Hwang, Phys. Rev., 180, 827 (1969)
24. E. W. Williams, A. M. White, Sol. State Comm., 9, 279, (1971)
25. H. Kressel, et al, J. Appl. Phys., 39, 2006 (1968)
26. C. J. Hwang, J. Appl. Phys., 38, 4811 (1967)
27. P. K. Chatterjee, et al, Sol. State Comm., 17, 1421 (1975)
28. S. Y. Chiang, G.L. Pearson, J. Appl. Phys., 46, 2986, (1975)
29. W. Y. Lum, H. Wieder, Appl. Phys. Letters., 31, 213 (1977)
30. W. Y. Lum, et al, Appl. Phys. Lttrs, 30, 1 (1977)
31. W. H. Koschel, et al, Inst. Phys. Conf. Ser No. 33a (1977), Ch 2
32. C. J. Hwang, J. Appl. Phys., 39, 5347 (1968)
33. L. L. Chang, L. Esaki, R. Tsu, Appl. Phys. Lttrs, 19, 143 (1971)
34. W. Spitzer, W. Allred, Appl. Phys. Lttrs., 12,5,(1968)
35. R. Romano-Moran, K. L. Ashley, J. Phys. Chem. Solids, 34, 427 (1973)
36. J. Gyulai, et al, Appl. Phys. Lttrs., 17, 332 (1970)
37. H. Bebb, R. Chapman, J. Phys. Chem. Solids, 28, 2087 (1967)
38. A. S. Grove, A. Leistiko, C. Sak, J. Phys. Chem. Solids, 25, 985 (1964)

ATE
LMED
— 8